EXPERIMENTAL INVESTIGATION OF A DOUBLE PASS SOLAR AIR HEATER HAVING RIBS AS ARTIFICIAL ROUGHNESS ON BOTH SIDES OF THE ABSORBER PLATE.

Dissertation-II

Submitted in partial fulfillment of the requirement for the award of degree

Of

Master of Technology

IN

MECHANICAL ENGINEERING

By

Prateek Minhas

(11510443)

Under the guidance of

Sudhanshu Dogra

(16900)

DEPARTMENT OF MECHANICAL ENGINEERING

LOVELY PROFESSIONAL UNIVERSITY

PUNJAB

CERTIFICATE

I hereby certify that the work being presented in the dissertation entitled “Experimental investigation of a Double Pass Solar Air Heater having ribs as artificial roughness on both sides of the absorber plate.” in partial fulfilment of the requirement of the award of the Degree of master of technology and submitted to the Department of Mechanical Engineering of Lovely Professional University, Phagwara, is an authentic record of my own work carried out under the supervision of Sudhanshu Dogra, Assistant Professor Department of Mechanical Engineering, Lovely Professional University. The matter embodied in this dissertation has not been submitted in part or full to any other University or Institute for the award of any degree.

(__.04.2017)

(Prateek Minhas)

(11510443)

This is to certify that the above statement made by the candidate is correct to the best of my knowledge.

(__.04.2017)

(Sudhanshu Dogra)

(16900)

COD (ME)

_____

_____The external viva-voce examination of the student was held on successfully _____

Signature of Examiner

ACKNOWLEDGEMENT

I have taken efforts in this pre-dissertation. However, it would not have been possible without the kind support and help of many individuals and organization. I would like to extend my sincere thanks to all of them.

I am highly indebted to **Mr. Sudhanshu Dogra** for his guidance and constant supervision as well as for providing necessary information regarding my thesis work & also for their support in discussing about the selected topic.

DECLARATION

I, ***PRATEEK MINHAS (11510443)***, hereby declare that this thesis report entitled "***Experimental investigation of a Double Pass Solar Air Heater having ribs as artificial roughness on both sides of the absorber plate***" submitted in the partial fulfilment of the requirements for the award of degree of Master of Mechanical Engineering, in the School of Mechanical Engineering, Lovely Professional University, Phagwara, is my own work. This matter embodied in this report has not been submitted in part or full to any other university or institute for the award of any degree.

Date: Prateek Minhas

Place:

TABLE OF CONTENTS

LIST OF TABLES

LIST OF FIGURES

ABSTRACT

Performance of the double pass solar air heater can be enhanced by increasing the heat transfer area. There are various methods used to enhance the performance of double pass solar air heater viz. using corrugated surfaces, extended surfaces, packed bed etc. The thermal efficiency of double pass solar air heater is more than the single pass solar air heater due to more heat transfer area. Based on the literature review, it is concluded that most of the studies are done on double pass solar air heater integrated with porous media and extended surface but less studies are done on corrugated surfaces. In order to enhance the thermal efficiency of a solar air heater artificial roughened surface on absorber plate considered to be an efficient technique. In various literatures it has been observed that the use of artificial roughened surfaces on the absorber plate can enhance the characteristics of Air heaters to a greater extent. The solar air heaters efficiency can be affected by various parameters such as collector length, number of channels, depth of channels, type of absorber plate, number and material of glass covers, air inlet temperature and air velocity.

CHAPTER - 1 INTRODUCTION

1.1 OVERVIEW

Based on the today's world scenario energy saving is one the major factors to maintain a stable economic growth the country. Energy can be renewable or non-renewable. Renewable is that form of energy that can be reused and are easily available in nature like solar energy, geothermal energy, wind energy etc. Non-renewable energy is that form of energy that is derived from fossil fuels like coal, petroleum. The non-renewable energy reservoirs are getting depleted with its usage. Research is going on renewable sources to replace these non-renewable energy sources. In developed countries like US, Russia etc are using the non-renewable energy sources in various form without the use of non-renewable energy. [1]

Energy is the major universal measure of work done of all types by nature and humans. Everything which occurs in this world is the expression of one form of energy flow. Many persons use the energy word for input to the machines and to their bodies. [1]

The sources of energy can be divided into three ways:

a) Primary Energy Sources: The sources which gives net energy flow are known as primary energy sources. Examples are Coal, Uranium, Oil etc. The energy needed to form these fuels is much less in comparison to the energy needed during combustion. The energy yield ratio is very high for these sources.

b) Secondary Energy Sources: The sources which does not produce any net energy are known as secondary energy sources. Their energy yield is less than the input. Examples are solar energy, tidal energy, water energy, wind energy, intensive agriculture etc.

c) Supplementary Energy Sources: The sources whose net energy yield is zero are known as supplementary energy sources. These sources need highest investment in terms of energy, Example is thermal insulation. [1]

Future of World Energy: At present the population of world is increasing at a very fast rate. If this rate continues the world will be heavily crowded in some years. The non-renewable sources of energy (coal, petrol, natural gas, wood etc.) are depleting at a very fast rate. Nuclear energy needs a very skilled labour along with safety. These are very hazardous and produce large amount of pollution. So there is a need to think towards the renewable energy sources. These sources are solar energy, tidal energy, wind energy etc. These sources are pollution free, and non-exhaustible in nature.

The amount of energy sources (in percentage) consumed by the world shown in the following table 1.1. [1]

Table 1.1: Percentage use of sources consumed by world [1].

Energy Sources	Percentage Utilization
Oil	38.3%
Coal	32.5%
Gas	19%
Wood	6.6%
Hydro	2.0%
Dung	1.2%
Waste	0.3%
Uranium	0.13%

1.2 RENEWABLE ENERGY SOURCES

Among all the renewable energy sources solar energy is the major source for the economic growth of the country. Solar energy is the major source having a potential of 178 billion

MW. It is about 20,000 times the world's demand. [1]. But still it could not be developed on a large scale. The energy from the Sun could be used as photovoltaic and thermal. Solar energy as thermal is being used for

i) steam

ii) hot water production.

Wind energy is another source of renewable energy. It requires certain locations where a minimum wind speed of 3 m/s is available. In USA a state named California is generating 500W energy. For generating such energy it requires 900 wind turbines. In various countries across the world around 0.7 million of wind pumps are in operation.

1.3 SOLAR ENERGY

Solar energy is most easily available form of renewable energy. The total energy received from the sun is around 35000 times the total energy used by man. The average intensity of solar radiation in India works out to be approximately 2000 kWh/m^2 as compared to the world average of 2500 kWh/m^2. But of the total solar energy reaching the earth's surface only 7-8% is being used, so there is a need to explore it and use it in a more efficient way. This energy source has been used for various applications for many years. The technologies developed from solar energy are classified into active solar and passive solar. Active solar techniques are that which involves the usage of photovoltaic systems and concentrated solar power to harness the solar energy. Passive techniques include the designing of space for natural air flow etc. Solar energy technology includes solar cookers, photovoltaic cell, solar air heater, solar collectors etc. These technologies are emerging in a rapid manner as this technologies are proved to save energy in many applications. In 1877 solar energy was utilized to heat a home.[1]

Some of the applications of solar energy are:

(1) Heating and cooling of residential building.

(2) Solar water heating.

(3) Solar drying of agricultural and animal products.

(4) Solar distillation on a small community scale.

(5) Salt production by evaporation of sea water or inland brines.

(6) Solar cookers.

(7) Solar engines for water pumping.

(8) Food refrigeration.

(9) Bio conversion and wind energy, which are indirect sources of solar energy.

(10) Solar furnaces.

Generally solar energy refers to the energy generated and transfer in the form of radiation from the Sun to the Earth. This energy can be directly or indirectly converted to other forms of energy. These forms are heat and electricity which can be used by human beings. The major disadvantages of application of solar energy are

i) the variable manner between Sun and Earth's surface
ii) the area required for collection of energy is very large.

SWOT analysis of solar energy [2]:

STRENGTH:

1. Never ending source of energy.
2. Pollution free.
3. Scope for decentralization.
4. Easy to operate.
5. Saves fossil fuel deposits.
6. Less hazardous.
7. Can be utilized in any form of energy.

WEAKNESS:

1. Problem for storage.
2. Not available in cloudy or eclipse days.
3. Initial investment is high.
4. Needs subsidy.
5. Spares not easily available.
6. Quantum varies according to seasons or weather.

7. Not yet taken on priority list.

OPPORTUNITY:

1. Scope for utilizing magnetic energy from solar wind.
2. Chance of hazard is less.
3. Scope of decentralization.
4. Totally pollution free.
5. Vast opportunity for expansion in many uses.

THREAT

1. Threat from oil lobby.
2. Threat from coal lobby.
3. Opposition from different forces due to subsidy.
4. Fluctuations due to season or weather may discourage consumers.
5. Lack of knowledge of common consumers.

Solar Constant

In Sun heat is generated by different fusion reactions. The diameter of the Sun is 1.39×10^{6} km. the diameter of Earth is 1.27×10^{4} km. The mean distance between Sun and Earth is 1.50×10^{8} km. At the Earth's surface an angle of only 32 minutes subtends by the Sun. The radiations (beam radiations) receiving by the Earth from the Sun is almost parallel. [3]. The Sun's brightness varies from its center to its edges. The standard value of the solar constant defined by the National Aeronautics and Space Administration (NASA) is given below:

1. 1.353 kilowatts per square meter.
2. 116.5 langleys (calories/m^2) per hour.
3. 429.2 BTU per square feet per hour.

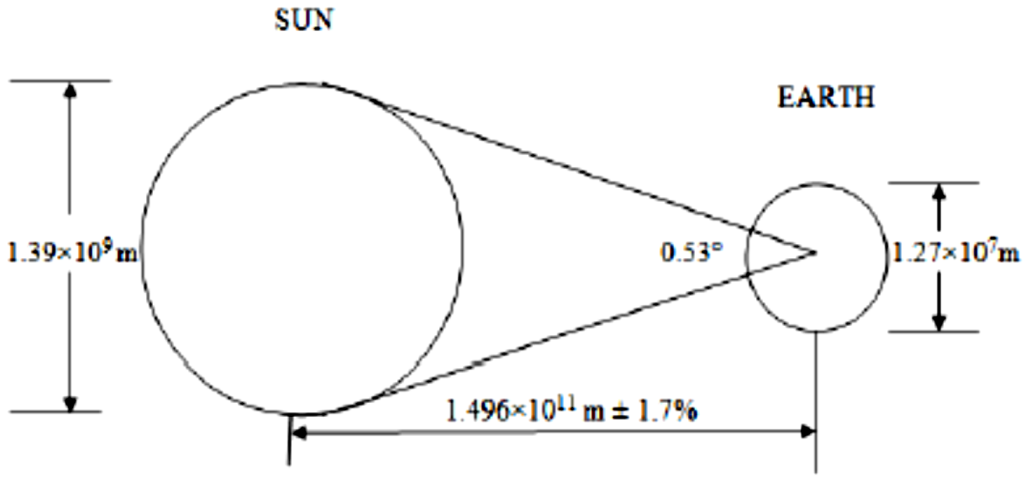

Figure 1.1: Relationship between the Sun and Earth [4].

The solar radiation reaches the Earth surface having three components. These components are given below:

1. Direct or Beam Radiations.
2. Diffuse Radiations.
3. Reflected Radiations.

Direct or Beam radiation (I_b): The radiations coming from the Sun penetrates the atmosphere of the earth and reach the surface of the earth. These amount and character of the radiations varies from top to the earth's surface. Some radiations are reflected back from the clouds [5]. Some radiations are absorbed partially by the air molecules. A solar radiation that reaches the surface directly without been absorbed or reflected back is termed as direct or beam radiation. It produces a shadow when comes in contact with an opaque object.

Diffuse radiation (I_d): When the solar radiations crosses through the earth's atmosphere, some of the radiation is absorbed by the air and water vapour. Some radiation gets scattered by air molecules, aerosols, dust particles and water vapours. This part of solar radiation which is scattered and absorbed is termed as diffuse radiation.

The total or global radiation (I) is given by:

$$I = I_b + I_d \qquad (1.1)$$

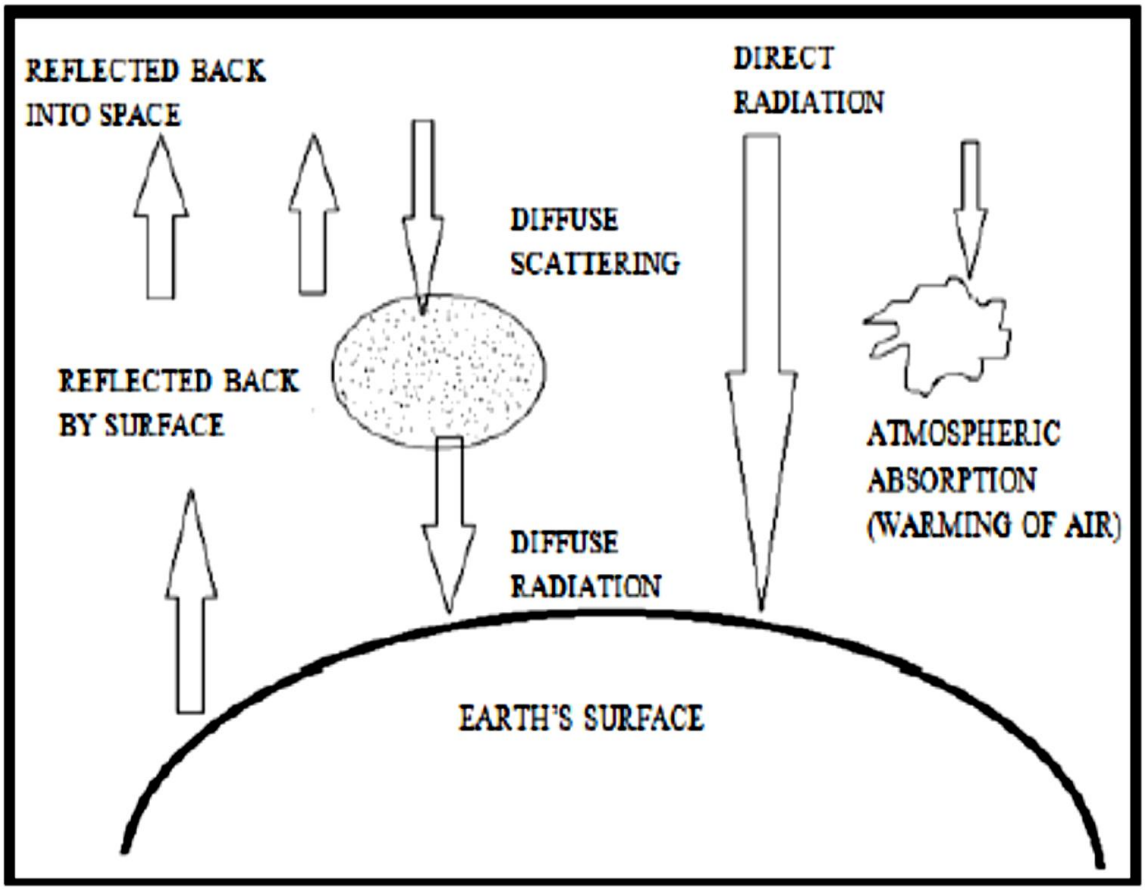

Figure 1.2: Direct radiations and Diffuse radiations [1].

1.4 SOLAR COLLECTORS

A device used to collect the radiations of the Sun and transfer this energy to a fluid passing in contact with it is called solar collector. Basically there are two types of solar collectors.

1. Non-concentrating or Flat plate solar collector.

2. Concentrating or focusing solar collector.

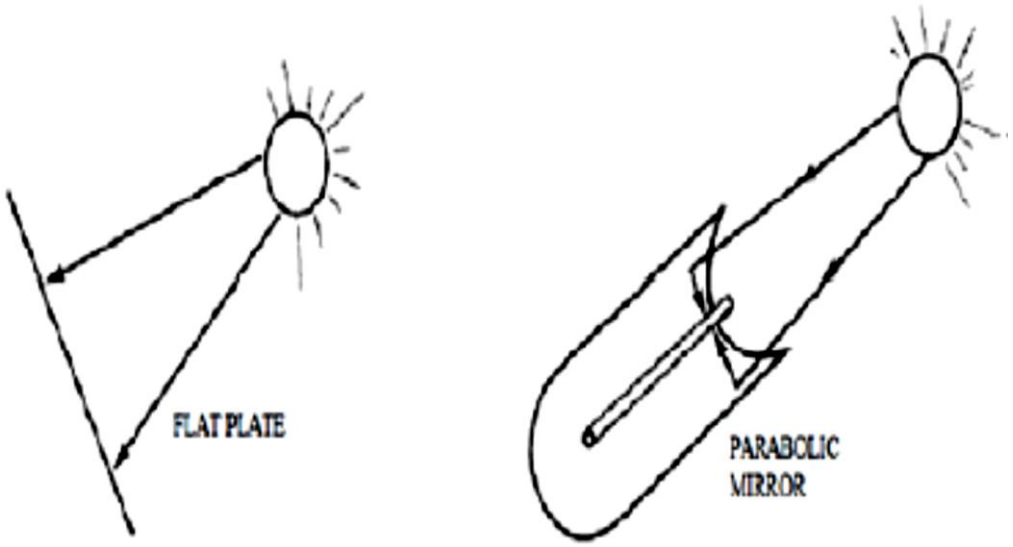

Figure 1.3: Flat and Parabolic type Collectors.

Table 1.2 shows that the various solar collectors along with the concentration ratio and there working temperature range.

Table 1.2: Solar collector types and their temperature range [4]

S. No.	Types of Collectors	Concentration Ratio	Typical Working Temperature Range (°C)
1	Flat Plate Collector	1	≤ 70
2.	High Efficiency Flat Plate Collector	1	70 – 120
3.	Fixed Concentrator	3 – 5	100 – 150
4.	Parabolic Trough Collector	10 – 50	150 – 350
5.	Parabolic Dish Collector	200 – 500	250 – 750
6.	Central Receiver	500 - >3000	500 - >1000

1.4.1 Flat Plate Collectors or Non-Concentrating Solar Collectors

Flat Plate collectors are for temperatures below 90°C are adequate. This is because they are used for water heating. These are made in rectangular panels. The area of panels are about 1.7 to 2.9 m^2. They generally collect both direct and diffuse solar radiations. Simple flat plate collector has a flat surface called as absorber plate which has high absorptivity for solar radiations [6]. An absorber plate is a metal plate painted with black colour to absorb the solar radiations. A heat transfer medium such as air is used to transfer the energy from the plate. The upper surface of the absorber plate is covered with a transparent cover like glass so that it transmits shorter wavelength solar radiations.

Flat plate collectors consist of five components:

1. A transparent cover such as glass.

2. Heat transfer medium such as tubes, fins, passage or channels which carry the fluid (air).

3. The absorber plate

4. Insulation on the back and sides this minimizes the heat losses.

5. The casing or container to enclose the other components.

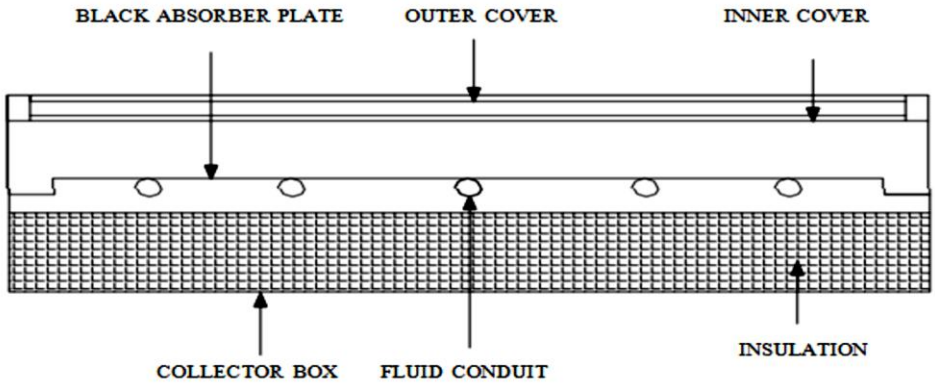

Figure 1.4: Flat plate collector [1].

On the basis of fluid of transfer of heat flat plate collectors are categorise in two types. These are:

(a) Liquid heating collectors.

(b) Air or Gas heating collectors.

a) Liquid heating collectors

A liquid heating collector consists of an absorbing surface which absorbs high solar radiation. Generally, a metal plate, of steel, copper or aluminium has been used along with the plate. The thickness of absorber 1 to 2 mm and tubes diameter ranges from 1 to 1.5 cm. Liquid stores in tank flows through tubes. This takes up the heat from the absorber plate. This heat returns to the tank. The application of flat type collectors are space heating, seasoning of timber, curing of industrial products, and crop drying.

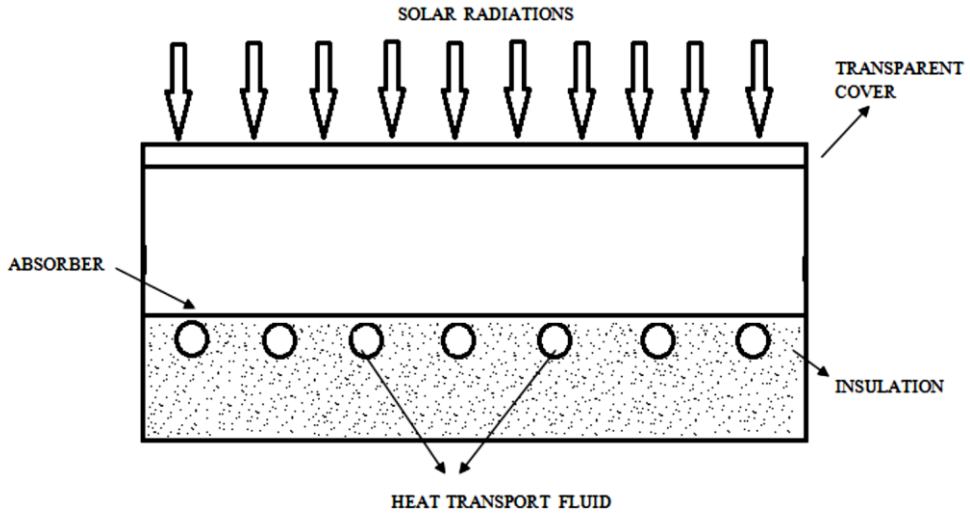

Figure 1.5: Liquid heating collector [1].

b) Air or Gas heating collectors:

Air/gas heating collectors are used widely because of their simplicity and less cost. These collectors are having various applications like crop drying, space heating, curing of industrial products and seasoning of timber. A typical flat plate air heating collector is shown in figure 1.6. Generally it includes an absorber plate. Another parallel plate along with absorber plate is placed below. The aspect ratio (W/H) is high.

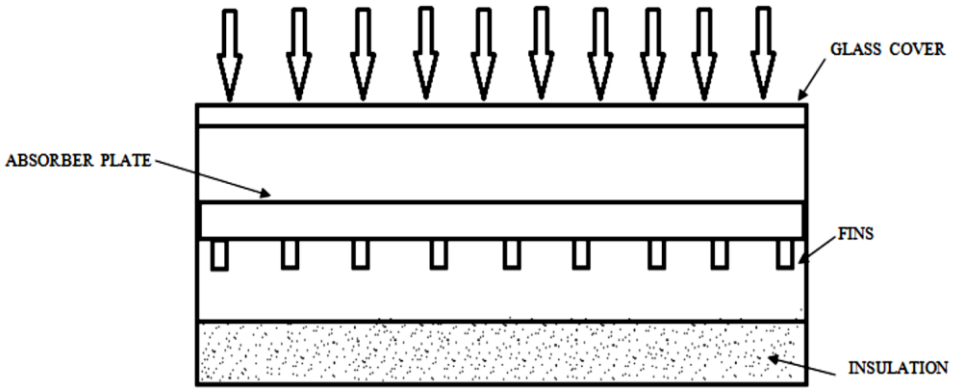

Figure 1.6: Solar air collector [1].

1.4.2 Focusing Collectors

Flat plate collectors obtained higher temperature are responsible for energy transmission in many applications. Delivery energy temperature is enhanced by reducing the area. This area is the area from which losses of heat takes place. This is achieved by using an optical device. This device is placed between the source of energy absorption and the radiation source. For similar absorbing temperature the heat losses are less for small absorber as compare to a flat plate collector. Due to this reason the concentrating collectors are used. Concentrating collectors collects the solar radiations from relatively large area and by using parabolic mirrors focus these rays on a point. A device which is used to collect high intensity solar radiation as solar energy on the surface of energy absorption is called as focussing collector.

Refractor or reflector is a form of optical system used by these collectors. It is a special modified form of flat plate collector by introducing a concentrator between the absorber and solar radiations. A focusing collector consist of

i) parabolic receiver
ii) cylindrical receiver
iii) spherical receiver.

Among these three receivers parabolic reflector gives high concentration from optical point of view.

An alternative is to use auxiliary mirrors to navigate the concentrator. These auxiliary mirrors are used to track the Sun and reflect the rays on to the parabolic concentrator. However some efficiency losses occur by using auxiliary mirrors. When high temperature required then these focusing collectors are used. Figure 1.7 shows the concentrating type solar collector.

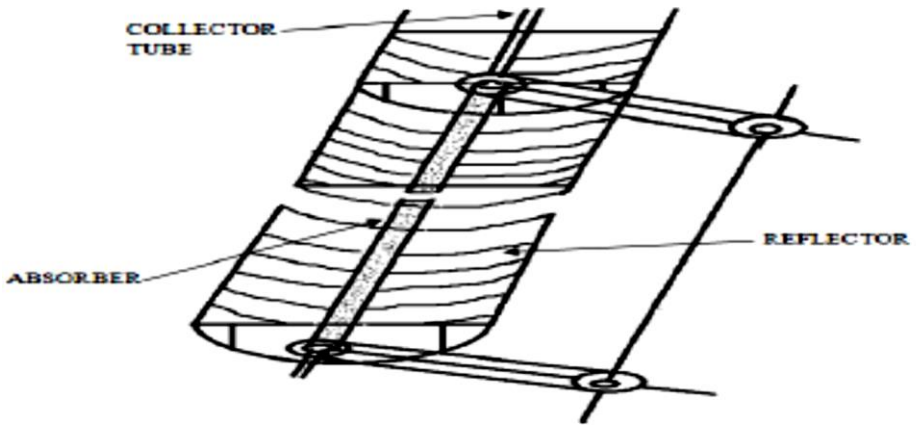

Figure 1.7: A Parabolic or concentrating type solar collector [1].

1.5 SOLAR AIR HEATERS

Air is used as a heat transfer medium in many of the energy conversion systems. Solar air heaters are made in different designs. In some of the absorber surface below the glazing includes

- overlapped glass plate,
- spaced glass plate,
- clear glass plate,
- black glass plates,
- single smooth metal sheets,
- flow through stacked screen or mesh,
- corrugated metal plates and others.

In other air passing below the plate. This air passage reduces downward heat loss. Figure 1.8 shows a sectional view of flat plate solar air heater.

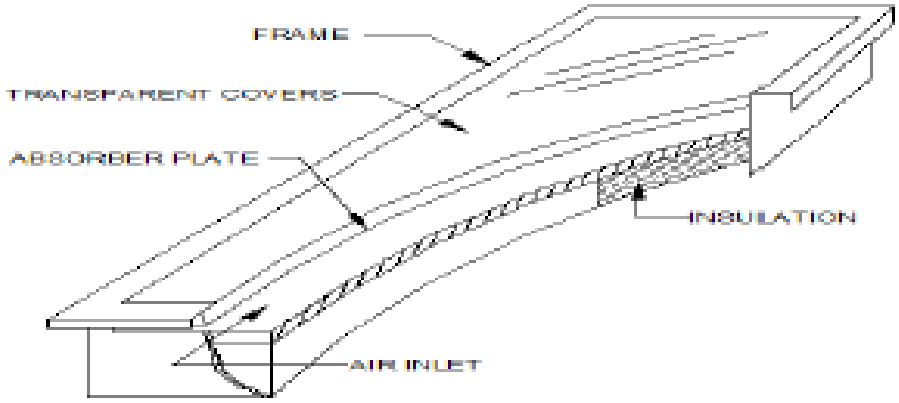

Figure 1.8: Flat plate solar air heater.

1.5.1 Simple flat plate collector

Simple flat plate collector is most commonly used. It includes of one or two glazing. It also includes insulation over the plate. The air flow may be either above or below or both the absorber plate. This is as shown in Figure 1.9.

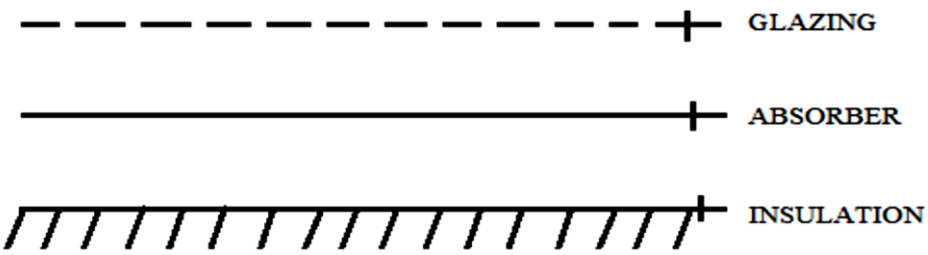

Figure 1.9: Simple flat plate collector [7].

1.5.2 Finned plate collector

This collector is modified type of the simple flat plate collector. Fins are used to increase the heat transfer coefficient. The fins are usually located in the air flow region. This is as shown in figure below.

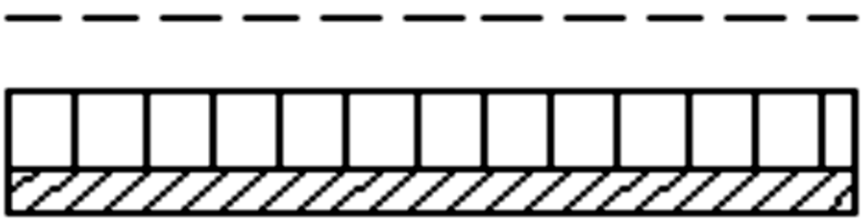

Figure 1.10: Finned plate collector [7].

1.5.3 Corrugated plate collector

The configuration of the simple flat plate collector is known as corrugated plate collector. The absorber is corrugated by rounded troughs or V-troughs. This configuration increases the heat transfer coefficient. This is as shown in Figure below.

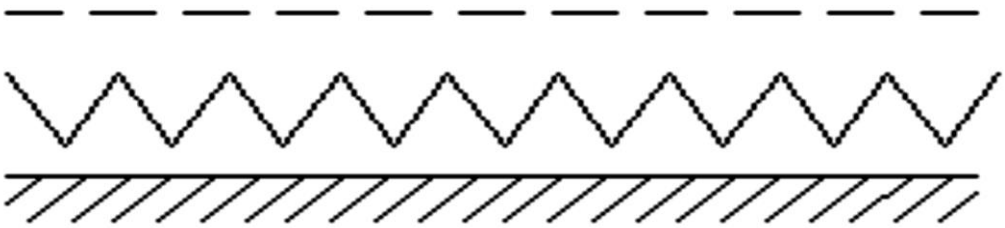

Figure 1.11: Corrugated plate collector [7].

1.5.4 Matrix type collector

An absorbing matrix is provided between the absorber plate and transparent cover. The matrix material may be the metal plate, or cotton gauge. This collectors gives high heat transfer to volume ratio. It may also give low friction losses. Figure 1.12.

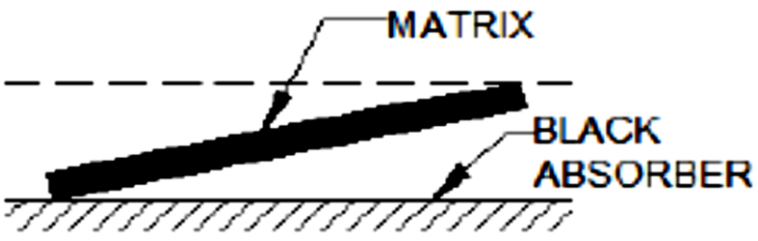

Figure 1.12: Matrix type collector [7].

1.5.5 Overlapped transparent plate type collector

This type of collector consist of a group of transparent plates. These plates are partially blackened. The bottom of unit is insulated. For moderate rise in temperature these collectors reflects good efficiencies. These collectors has a low pressure drop. Figure 1.13 shows overlapped transparent plate type collector.

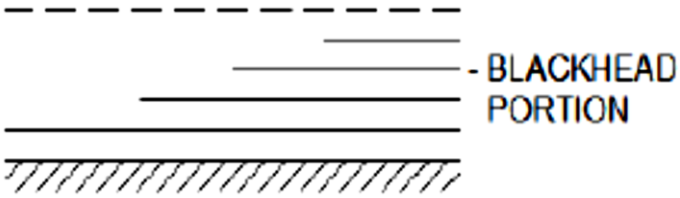

Figure 1.13: Overlapped transparent plate type collector [7]

1.5.6 Transpiration collector

It is a modified design of overlapped transparent plate type collector. The black absorber plate is replaced by closely packed matrix material. The air enters just under the innermost cover. This air is then flows downward through the porous bed. This air is then distributed in the distributing ducting. Figure 1.14 shows the transpiration collector.

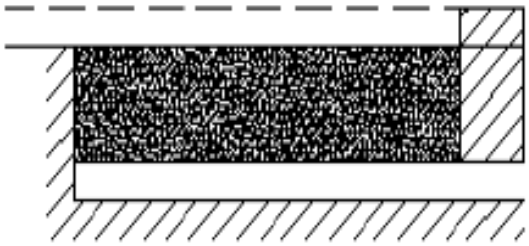

Figure 1.14: Transpiration collector [7]

1.5.7 Bare air type solar collector

It consist of an air duct with an absorber plate in uppermost surface. Heat transfer through the back side of absorber plate. This heat transfer to the air stream from absorber platre. Figure 1.15 shows a simple bare type solar collector.

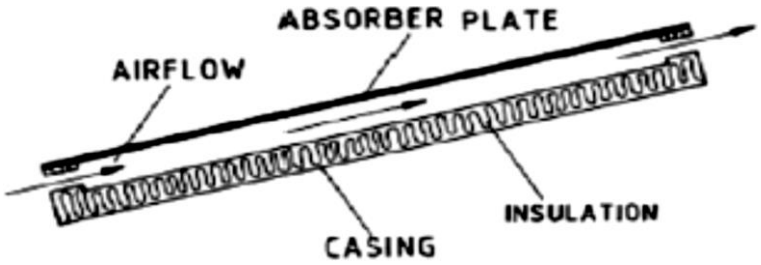

Figure 1.15: A bare air type solar collector [6].

1.5.8 Covered type air solar collector

To minimize the heat losses from upper side one or more glass covers are used. This type of collector is called as Covered Plate Air type Solar Collector. This cover protects the absorber plate from external effects. There are 4 types of such collectors.

i) Front Pass Covered Plate Air Type Collector.
ii) Back Pass Covered Plate Air Type Collector.
iii) Suspended Plate Covered Plate Air Type Collector.
iv) Perforated Plate Covered Plate Air Type Collector.

Figure 1.16 shows covered type solar air collector.

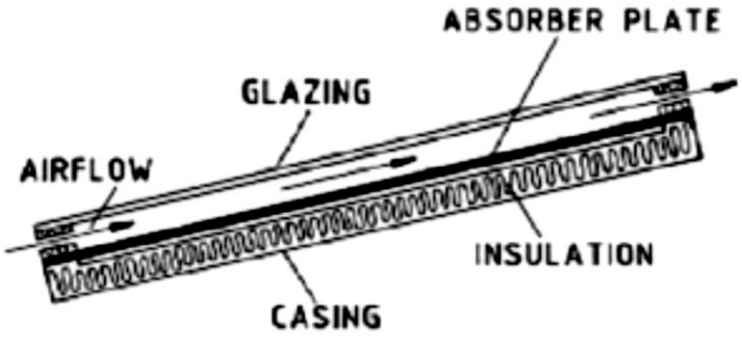

Figure 1.16: Covered type solar air collector [6].

1.5.9 Perforated Plate Covered Plate Air Type Solar Collector

It is a modified form of suspended plate air type solar collector. It is also known as matrix solar heater. Blackened gauze which is a porous high surface area absorber is used to make such type of collector. This type of collector has an advantage of more efficiency as compare to the other. This is because of greater heat transfer coefficient and greater surface area. It has certain disadvantages which are:

i) high pressure drop
ii) high technical stress on absorber.

Figure 1.17 shows this type of air collector.

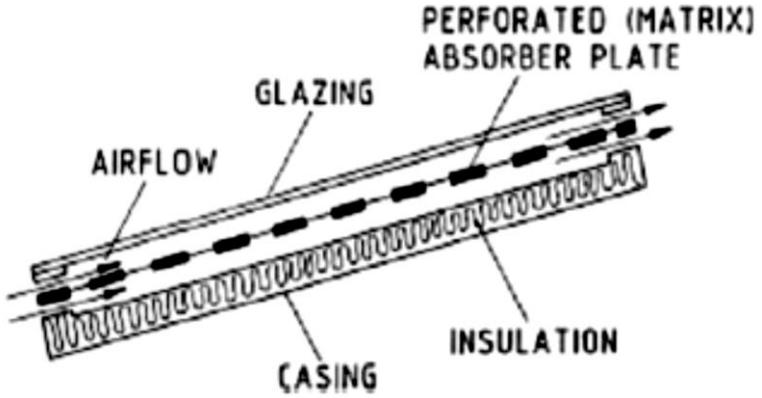

Figure 1.17: Perforated plate covered plate air type solar collector [6].

1.5.10 Two-pass solar air heater

To reduce the losses in two pass solar air heater as suggested by Satcunanathan and Deonarine.[8] The air first passed between the covers of a two glass cover heater and then under the absorber plate as shown in Figure below. This results in reduction of outlet glass cover temperature by 2-5°C. This results in reduction of the losses and the efficiency of the collector is increased by 10 to 15% than a conventional heater.

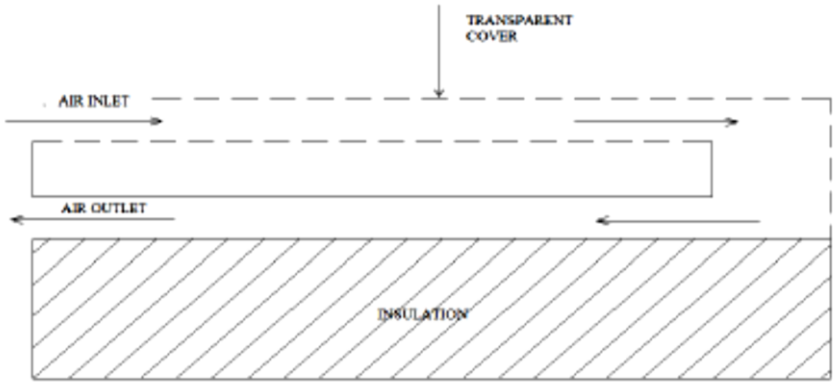

Figure 1.18: Double Pass Solar Air Heater [8].

1.6 Performance Enhancement Techniques For Solar Air Heaters

The performance can be enhanced in many ways. The following are some techniques to enhance the performance of solar air heaters.

1.6.1 Reduction of heat losses

Heat loss is one of the main reason for low heat transfer which further effects the efficiency of the heater. Minimization of heat loss, increases the properties of solar heater. The ways of reducing heat losses are discussed below.

1.6.1.1 By lowering convective as well as radiative heat losses

Two or more glass covers are used to reduce the convective and radiative heat losses when operated at moderately high temperatures. Surface treatment is used to reduce glass reflectance. Glass cover transmits solar radiations having lower wavelengths and eliminates radiations with higher wavelengths.

1.6.1.2 By Using Alternate Medium or Vacuum in the Gap Space

By Optimization of the gap space minimizes the convective heat losses. Malhotra et. al. [9-10] investigated that reduction of heat losses up to 34% can be achieved by the use of heavy gases. It was reported that using a combination increases the daily energy collection by 278% and thus making the collector to operate at 150°C. A daily energy collection efficiency more than 40%.

1.6.1.3 By Selective Absorber Surfaces

When the temperature of the absorber plate is very high from the ambient air temperature then the selective surfaces plays an important role. Usually large amount of heat loss occurs from the absorber surface. At wavelength of about 10 microns, maximum radiation loss appears. Maximum solar energy absorbed by the absorber plate is between 0.3 microns and 2.5 microns .This results in increase in efficiency of solar collector. Also makes it possible to achieve higher temperature.

1.6.2 Improvement of Heat Transfer from Absorber Plate

High absorber plate temperature with high heat losses to the environment can be achieved by using low convective rate of heat transfer. This rate is between the absorber plate and the duct air. By reducing the temperature of the plate losses can be reduced. The absorber

plate temperature is reduced by increasing the heat transfer coefficient. This coefficient is between the absorber plate and the duct air. This can be achieved by following methods.

1.6.2.1 By Providing Packed Bed Absorbers for Solar Air Heating Collectors

The major disadvantage of this type of collector includes the high initial cost and large pumping power requirement in comparison to simple solar air heaters.

1.6.2.2 By Increasing the Area of Heat Transfer without Effecting the Convective Heat Transfer Coefficient

Surfaces that are used to increase heat transfer area are called extended surfaces fins. Bevill and Brandt [11] explains a solar air collector which includes 96 aluminium fins. These fins were arranged parallel. The spacing between these fins were uniform. These are kept beneath the glass cover. The collector was designed in such a way to obtain high collector efficiency, low pumping power to pass air through the collector. The result shows that more than 80% of the efficiency is achieved.

1.6.2.3 By Increasing Convective Heat Transfer Coefficient using Artificial Roughness

The flow at the turbulent heat transfer surface result in high convective heat transfer co-efficient. The energy for creation of turbulence is derived from the fan or the blower. The excessive turbulence means excessive power requirement. So it is desirable that turbulence must be created close to the surface. In laminar sub layer only, so that the heat exchange takes place and the core of the flow is not unduly disturbed to avoid excessive losses. This can be achieved by using roughened surfaces on the air side. Usage of artificial roughness improves the coefficient of heat transfer.

1.6.3 Thermohydraulic performance of solar air heaters

The introduction of artificial roughness on the rear side of the absorber plate results in high heat transfer co-efficient. This leads to high collection efficiency. Consideration of artificial roughness enhances the thermal performance of solar air heaters. This results in high friction factor and a high pumping power. So optimization of the system is required to maximize the thermal exchange. The friction losses should be at the minimum possible level.

The effective efficiency is

$$\eta_{th} = \frac{q_u - \frac{P_m}{C}}{IA_c} \quad (1.1)$$

CHAPTER – 2 SCOPE OF STUDY

The future scope of this research study are for following applications:

- Heating and cooling of residential building.
- Solar water heating.
- Solar drying of agricultural and animal products.
- Solar distillation on a small community scale.
- Salt production by evaporation of sea water or inland brines.
- Solar cookers.
- Solar engines for water pumping.
- Food refrigeration.
- Bio conversion and wind energy, which are indirect sources of solar energy.
- Solar furnaces.

CHAPTER – 3 OBJECTIVE OF STUDY

- The main objective is to enhance the rate of heat transfer.

- To improve the efficiency of double pass solar air heater and compare the obtained results with the single pass solar air heater.

- To achieve such results W-shaped ribs are attached to the absorber plate so that the heat absorption capacity is increased.

- To investigate the Nusselt number and friction factor and also compare with the results obtained for single pass solar air heater.

- To find out thermal and thermo-hydraulic efficiency based on hydraulic diameter.

CHAPTER – 4 REVIEW OF LITERATURE

A comprehensive purpose of literature review is to get background information regarding the problems to be considered during present study. The article includes the brief review on the methods adopted for the enhancement or increase the heat transfer. One of the various techniques which considered to rise the forced convection heat transfer. The flow should be turbulent closer to the surface of the heat transfer to get higher heat transfer coefficient. However, blower or fan give the energy required to generate such turbulence. The excessive turbulence results in excessive requirement of power for flow of air through duct. So, it is required to minimise such loss of power to increase its efficiency.

Because of this roughness, generation of turbulent boundary layer along with little laminar sub-layer occurred on the surface of absorber plate. Very high resistance offer to the flow of heat due to this laminar sub-layer. The characteristics of heat transfer rate and the friction factor can be improved by breaking laminar sub-layer. It is further enhances the thermo-hydraulic performance and the thermal efficiency of solar air heater.

Abhishek Saxena et. al. [12] investigated the design and performance of a solar air heater with long term heat storage. The main objective of this is to increase the heat transfer rate and to raise the efficiency of simple solar air heater. He introduced an absorbing media i.e. granular carbon inside solar heater. The calculation of thermal performance of solar heater had been done on four distinct arrangement of parts or elements by operating it on both natural and forced convection. He designed and fabricated two solar air heaters (s1 and s2) of identical particular dimensions to offer hot air for space heating and drying. It was reported that for ‘s1’ the maximum efficiencies were 16.16%, 19.02%, 17.04%, and 18.16% on natural convection for four distinct arrangements while for ‘s2’ the maximum efficiencies were 17.79%, 20.77%, 18.27%, and 18.95% on similar arrangements of parts and elements on natural convection and the maximum efficiencies for ‘s1’were 39.5%, 46.51%, 53.05%, and 56.91% while for ‘s2’ were 43.14%, 53.97%, 55.64%, and 73.65% on similar arrangements of parts on forced convections.

Sukhmeet Singh et. al. [13] investigated the correlations of friction factor and heat transfer of solar air heater with discrete V – down ribs as artificial roughness on the absorber plate.

He examined the rectangular duct heated the one wide wall and artificial roughness provided as V – down ribs subjected to consistent heat flux which is having Reynold Number (Re) shifted from 3000 – 15000, with relative gap position (d/w) = 0.20 – 0.8, and relative gap width (g/e) = 0.5 – 2.0, angle of attack (α) = 30° - 75°, relative roughness pitch (P/e) = 4 – 12, and relative roughness height (e/D_h) = 0.015 – 0.043. It was reported that maximum increment in Nusselt number (Nu) is 3.04 and maximum increment in friction factor (f) is 3.11 when contrasted with smooth pipe. It was likewise reported that in the scope of parameters concentrated, these correlation foresee the estimations of f and Nu with average absolute variation of 2.1% and 3.1% respectively.

Sharad Kumar et. al. [14] investigated the performance of a solar air heater based on CFD. He used an arc shaped geometry made up of thin circular wire as artificial roughness. It was analysed that the impact of arc shaped geometry on friction factor, heat transfer coefficient, and performance increment was examined covering the scope of roughness parameters (Re from 6000 to 18000, e/D from 0.0299 to 0.0426, solar radiation of 1000 W/m², α/90 from 0.333 to 0.666). The ribs (arc shaped wires) are given on one side of absorber plate and opposite side kept smooth. It was reported that Nu increases as the Re increases. While friction factor decreases as the Re increases for all assemblage of α/90 and e/D and the maximum value of overall enhancement ratio is 1.7 for roughness geometry related to e/D of 0.0426 and α/90 of 0.333for the scope of parameters considered.

S.K. Singal et. al. [15] investigated experimentally the thermal performance of solar air heater with roughness element in the form of blend of inclined ribs and transverse ribs attached on the absorber plate. It was examined that blend of transverse ribs and inclined ribs attached on the absorber plate with parameters such as Re scopes from 2000 to 14000, e = 1.6 mm, W/H = 10, P/e = 3 – 8, P = 5 – 13 mm, e/D_h = 0.030 for examination to concentrate the friction characteristics and heat transfer. The heat transfer and friction characteristics first calculated and then compared with the smooth duct. It was reported that under same stream conditions the geometry with P/e value of 8 results in maximum thermal efficiency. Further it was also accounted for that the maximum heat transfer coefficient found for the best thermal performance.

Brij Bhushan et. al. [16] investigated the correlations of Nusselt number and friction factor (f) for solar air heater with roughness element in the form of protrusions/dimples applied on the absorber plate. It was examined that so as to foresee execution of the framework

having such sort of roughened absorber plate, correlations of Nusselt number and friction factor as a function of framework and working parameters have been produced by utilizing trial information. It was reported that maximum increment in Nusselt number and friction factor had been found 3.8 and 2.2 times separately in contrast with smooth duct for the examined scope of parameters and the most extreme increment in heat transfer coefficient had been found to happen for S/e of 31.25, L/e of 31.25 and d/D of 0.294.

M. Samiev [17] investigated the solar air heating collector for finding the efficiency using a very simple moving plate heating model. It was reported that the static efficiency η can be about 0.5 for surrounding air temperature t_a = 40°C, for t_a value of 50°C the η is around 0.45, and t_a value of 60°C the η is around 0.37.

Prashant Dhiman et.al. [18] investigated analytically the solar air heater having packed bed roughness element placed in a novel parallel stream for finding out the thermal performance. A mathematical model was developed for analysing the solar heater thermal performance, and calculated by utilizing a developed PC code that uses an iterative arrangement method. It was reported that the difference between the results after simulation and exploratory information with a mean blunder of 9.2%, and the created mathematical model gives reasonable expectations of the execution of a PFPBSAH and can be a helpful design device for future advancement to fulfill particular applications.

Kaushik Patel et. al. [19] investigated the double pass solar air heater by utilizing baffles and longitudinal fins to increase the thermal performance. This investigate study is a near investigation of metallic wiry sponge to the baffles and longitudinal fins embedded inside the double pass solar air heater. It was reported that the maximum sun based radiation got in the metallic wiry sponge type double pass solar air heater when contrasted with the solar air heater with baffles and longitudinal fins and the greatest effectiveness had been picked up in the double pass solar air heater with metallic wiry sponge when contrasted with the other.

Sunil Chamoli et. al. [20] investigated the double pass solar air heater using absorber plate artificially roughened from both sides to enhance the performance. It incorporates the heat transfer increment, design of double pass solar air heater, pressure drop, and flow phenomenon in duct. The double pass solar air heater's performance and the different techniques those misrepresent their performance and numerical models of a few designs of

double pass solar air heaters are explored both experimentally and analytically. It was reported that there is enormous scope for future investigation of double pass solar air heater coordinated with roughness element on absorber plate surface on both upper and lower side. The most extreme efficiency is acquired if the duct depths and mass flow rate of air is similar in both the upper duct and lower duct.

Kaushik Patel et. al. [21] investigated the double pass solar air heater using fins, baffles and porous media to improve the thermal efficiency and determined the impact of various kind of media on the efficiency of double pass solar air heater. The impacts of major parameters air velocity, temperature difference, mass flow rate, pressure difference of the air had been watched for these perform contemplate. It was reported that the maximum efficiency was observed when the absorber material uncoated metallic wiry sponge in the solar still. It was lower cost effective and availability in the market was easy.

Anil Kumar [22] investigated the double pass solar air heater's performance having artificial roughness using CFD. The roughness geometries used were V-shaped thin circular wire, Multi V-shaped ribs and Multi V-shaped ribs with gap. The roughness parameters are as relative roughness width (W/w) value 6, relative gap width (g/e) is 1.0, relative gap distance (G_d/L_v) is 0.69, aspect ratio (W/H) is 12, relative roughness height (e/D) is 0.043, relative roughness pitch (P/e) is 10, and angle of attack (α) is 60°. It was reported that the increment in heat transfer is observed to be expanded to 1.7 times with that of the heat transfer of seamless surface for V-shaped, increased to 4.7 times for multi V-shaped and 5.6 times for Multi V-shaped with gap ribs.

Pongjet Promvonge et. al. [23] investigated the solar air heater for the thermal performance of turbulent channel flows over absorber plate having triangular (isosceles), wedge (right-triangular) and rectangular shaped ribs. The main aim of this study was to develop the experimental data accessible on different triangular rib shapes (i.e. right-triangular and isosceles) with comparable e/H proportion of 0.3 placed on a high aspect ratio duct having turbulent duct flows in a scope of 4000 to 16000. It was reported that the staggered triangular rib ought to be connected rather than the rectangular one to acquire higher heat transfer and thermal performance of around 50–65%, prompting to more short heat exchanger and the best working administration for all rib turbulators was found at the most reduced Reynolds number values.

R. P. Saini et. al. [24] investigated experimentally the solar air heater with arc shaped wire as roughness for the development of correlations for Nusselt number and friction factor so as to enhance the heat transfer coefficient. The flow of air in the duct was taken parallel for this investigation. It was reported that the most extreme increment in Nusselt number had been calculated as 3.80 times circumstances comparing the relative arc angle (α/90) = 0.3333 at relative roughness height = 0.0422, the enhancement in friction factor was 1.75 times only comparing to these parameters had been noted.

Subhash Chander et. al. [25] investigated the solar air heater with multi-gap V-down ribs along with staggered ribs attached on one side of the absorber plate as roughness element for examine the friction factor, heat transfer, and thermo-hydraulic performance properties of stream in a rectangular duct. The rectangular duct with Re scope from 4000 to 12000, aspect proportion of 12, rib height to hydraulic diameter (e/D_h) proportion from 0.026 to 0.057, rib pitch to height (P/e) proportion scope from 4 to 14, angle of attack (α) scope from 40° to 80°, staggered rib length to rib height proportion (w/e) = 4.5, gap width to rib height (g/e) proportion = 1, relative staggered rib pitch (p/P) = 0.65 and 2 number of gap (n) placed on each side of V-leg were used. It was reported that the 2 peaks for Nusselt number related to the P/e of 6 and 12 and decrement in the Nusselt number was noted for increment in the e/D_h more than 0.044 and the maximum increment reached in Nusselt number and thermo-hydraulic performance was of 3.34 and 2.45 times separately.

Ravi Kant Ravi et. al. [26] investigated the double pass solar air heaters (DPSAHs) for various methods used for the enhancement of the performance. The performance of a traditional solar air heater (SAH) can be adequately improved by diminishing the misfortunes from the collector surface by giving the best possible insulation and expanding the convective coefficient between working fluid and heat collecting surface by increasing the heat transfer area. This heat transfer area can be enhanced by double pass design. He utilized packed bed materials (PBMs), corrugated absorbing surfaces, and extended surfaces. The aim of this research was to review various heat transfer increment methods utilized in DPSAHs. It was reported that the recycling concept can be utilized to improve the thermal efficiency of DPSAHs. It was likewise reported that in case of finned DPSAH, number and orientation of the fins, fin height were found to be the critical parameters and in the event of artificially roughened DPSAH, roughness geometry and height, and fin height was considered as the imperative parameters.

Satyender Singh et. al. [27] investigated the double pass solar air heater with packed bed as roughness element for the increment of thermal performance. The material used in this investigation was porous packed bed in the upper duct of double pass solar air heaters. The thermal performance increases significantly in comparison with packed bed when porous material is applied in the lower channel and solar air heaters except packed bed. A wide literature review of double channel DPSAH had been displayed in this study with a goal to stress the significance of double duct double pass packed bed solar air heaters. It was reported that that there is significant ascent in the heat transfer coefficient with packed bed solar air heaters and thus, enhance thermal efficiency. It was likely reported that the hypothetical and exploratory reviews show that the double pass for example counter and parallel flow packed bed solar air heater work superior to the single pass packed bed solar air heaters attributable to the decreased thermal misfortunes from the intro and back surfaces of double duct system.

K. Kalidasa Murugavel et. al. [28] investigated experimentally the double pass solar air heater with storage of thermal energy. Paraffin wax in aluminium round and hollow (cylindrical) capsules was utilized as a medium of thermal storage on the absorber plate. The experimental study was led to assess the performance of the DPSAH with different setups under the metrological atmosphere of K.R. Nagar (9°11'N, 77°52'E) which is in the state Tamil Nadu, India. It was reported that the paraffin wax as energy storing material in solar air heater transfers nearly high temperature air for the duration of the day and additionally the efficiency is also higher amid evening hours and the capsules placed on the absorber plate of double pass solar air heater was the efficient one.

Nima Mirzaei et. al. [29] investigated the solar air heater for finding the best arrangement by outline and examination of try different things with single pass and double pass solar air collectors with wire mesh layers and ordinary and punctured covers rather than an absorber plate. The porous media were placed in a way that it reaches a high porosity (0.83) and a small pressure drop around the collector. The main purpose of this study was to tentatively explore the performance of solar air heater and recommend the arrangement which prompts to the maximum thermal efficiency. The design and investigation of experimental technique are utilized to frame the same solar based collector and the information was dissected with IBM's Statistical Package for the Social Sciences (SPSS) software. The most extreme average efficiency was reported to be 54.8% at a value of mass

flow rate was 0.032 kg/s. This was acquired from the double pass collector with a quarter perforated 10D cover, while the most extreme mean thermal efficiency got from the counter-flow collector with a typical Plexiglas cover was found to be 50.9% at the similar flow rate.

Raheleh Nowzaria et. al. [30] investigated experimentally the double pass solar air heater in which absorber plate was exchanged with 14 steel wire mesh layers (cross section of 0.2 × 0.2 cm) opening, and were fixed in the channel which was parallel to the glazing. The separation between every arrangement of wire mesh layers was 0.5 cm to minimize the drop in pressure. The black paint was applied on wire mesh layers before introducing them inside the collector. It was reported that the maximum temperature gradient (ΔT) (53°C) was accomplished at the rate of flow = 0.011 kg/s and the mean efficiency got for the double pass solar air collector with height of channel of 3 cm was 53.7% for the value of mass flow rate = 0.037 kg/s.

S. M. Shalaby et. al. [31] investigated theoretically and experimentally the double pass finned solar air heaters (DPFIPSAH) and V-shaped corrugated absorber plate (DPVCPSAH) for the thermal performance by the mode of heat transfer i.e. forced convection. Mathematical model was performed for calculating the enhancement in the thermal properties. Various measurements and comparisons were done like outlet temperature of air stream, absorber plate temperature, double pass finned power at outlet. It was reported that the DPVCPSAH was more efficient from the range of 9.3 to 11.9% as compared to DPFIPSAH, there was enhancement in thermal efficiencies of DPFIPSAH and DPVCPSAH with increment in mass flow rate value until it reached to 0.04 kg/s, past which, the expansion in thermal efficiencies of both of two systems were irrelevant, the thermo hydraulic efficiency of the DPVCPSAH having maximum value of 17.4% more as compared to that of the DPFIPSAH, the ideal estimations of the thermo hydraulic efficiencies of the DPVCPSAH and DPFIPSAH were found when the mass flow rates of the streaming air equal 0.0225 and 0.0125 kg/s, respectively.

L. B. Y. Aldabbagh et. al. [32] investigated experimentally the single and double pass solar air heater with roughness element as fin attached and utilizing a steel wire mesh on absorber plate for finding the thermal performance. The impacts of mass flow rate of air on the thermal efficiency and exit temperature ranges between 0.012 kg/s and 0.038 kg/s was studied. The utilized porous media comprise of steel wire mesh layers placed in an

arrangement from base to top at a distance of 1 cm above one another to give high porosity and to lessen the drop in pressure over the solar air heater. To expand the surface region of the collector the longitudinal fins were introduced and settled along the upper and lower passage of the solar air heater. The second point of this work was to explore the impact of the primary passage height of solar air heater on the thermal performance. It was reported that for both single pass and double pass solar air heaters for the constant mass flow rate of air = 0.038kg/s the greatest thermal efficiency got was 59.62% and 63.74% respectively.

Table 4.1: Literature review chart for findings in various investigations:

Investigator	**Solar Air Heater System**	**Findings**
Prashant et. al. [18]	Parallel Flow Solar Air Heater	It was concluded that the correlation between the simulation solution and test information with a mean error of 9.2% and this numerical model gives sensible forecasts of the execution of PFPBSAH and can be a helpful design plan device for future advancement to fulfill particular applications.
Avdhesh Sharma et. al. [33]	Double Pass Solar Air Heater having 'V' shaped roughness on absorber plate.	It was concluded that the increment in the heat transfer by applying artificial roughness on all the sides of absorber plate and the most extreme value of heat transfer increment observed to be 1.7 times when compared to the pipe with smooth surface and the increment in the friction factor found to be 1.9 times as compared to the pipe with smooth surfaces.

Raheleh Nowzari et. al. [30]	Double Pass Solar Air Heater with Wire Mesh Layer on the Absorber Plate	It was concluded that the fractional uncertainty of the efficiency and the mass flow rate was observed to be 0.0079 and 0.0033, separately. It was likely reported that the mean efficiency got was 53.7% for the double pass air collector for the value of mass flow rate of 0.037 kg/s.
A.A. El-Sebaii et. al. [34]	Double Pass Solar Air Heater with Packed Bed	It was concluded that the enhancement in thermo-hydraulic efficiency η_{th} with increasing $\dot{m}_f$ until a typical value of 0.05 kg/s beyond which the increment in η_{th} becomes inappropriate. It was likely concluded that gravel provided slightly improvement in performance as compared to limestone.
Brij Bhushan et. al. [35]	Solar air heater duct having protrusions as roughness geometry	It was reported that maximum increment in Nusselt number and friction factor had been found 3.8 and 2.2 times separately in contrast with smooth duct for the examined scope of parameters and the most extreme increment in heat transfer coefficient had been found to happen for S/e of 31.25, L/e of 31.25 and d/D of 0.294.
R. P. Saini et. al. [24]	Solar Air Heater having arc-shape parallel wire as roughness element	It was reported that the most extreme increment in Nusselt number had been calculated as 3.80 times circumstances comparing the relative arc angle (α/90) = 0.3333 at relative

		roughness height = 0.0422, the enhancement in friction factor was 1.75 times only comparing to these parameters had been noted.
Dinkar Prasad Singh et. al. [36]	Double Pass Solar Air Heater having discrete ribs on absorber plate	It was concluded that with increment in the Reynolds number both thermo-hydraulic and thermal efficiencies also increases and achieved the most extreme value at relative roughness pitch = 10 and after applying ribs the efficiencies were 1.3 times as compared to the surface of smooth plate.
Satcunanathan et. al. [8]	Counter Flow Solar Heater	It was concluded that the solar air heater having ordinary two glass cover solar air heater can be worked as a double pass solar air heater by before the air passing black end collector the air initially pass in the gap between the glass panes. It was noted that the output was proper rectification in the execution of the collector. This rectification was got at no increment in the unit cost.
Subhash Chander et. al. [25]	Solar Air Heater with multi-gap V-down ribs combined with staggered ribs	It was reported that the 2 peaks for Nusselt number related to the P/e of 6 and 12 and decrement in the Nusselt number was noted for increment in the e/D_h more than 0.044 and the maximum increment reached in Nusselt number and thermo-hydraulic

		performance was of 3.34 and 2.45 times separately.
Kaushik Patel et. al. [19]	Comparison of Double Pass Solar Air Heater with Solar Air Heater with Baffles and with Longitudinal Fins	It was reported that the maximum sun based radiation got in the metallic wiry sponge type double pass solar air heater when contrasted with the solar air heater with baffles and longitudinal fins and the greatest effectiveness had been picked up in the double pass solar air heater with metallic wiry sponge when contrasted with the other.
S.K. Singal et. al. [15]	Comparison of Double Pass Solar Air Heater with Solar Air Heater with Baffles and with Longitudinal Fins	It was concluded that the roughness element geometry having relative roughness pitch value of 8 had the most extreme thermal efficiency. It was likely concluded that the recommend way of operation can be successfully used for forecasting the performance of solar air heating.

CHAPTER – 5 EQUIPMENT, MATERIAL, AND EXPERIMENTAL SET-UP

5.1 INTRODUCTION

It can be said from the literature review that the application of artificial roughness on the absorber plate which is used in solar air heater enhances the thermal performances. The artificial roughness on the absorber plate increases the heat transfer coefficient and the friction factor. Various studies have been going on single pass and double pass solar air heater to display the impact on the heat transfer enhancement. The enhancement can be made by adding artificial roughness. The artificial roughness has been provided by using inserted tapes, machining, ribs, etc. Various investigators concluded that ribs glued is one of the effective methods to develop artificial roughness. The different shapes like inclined, transverse, V, W etc. developed glued over the surface of the absorber plate to increase the heat flow rate as well as friction factor.

5.2 EXPERIMENTAL SET-UP

Fig. 5.1 shows a schematic diagram of the experimental set-up. The experimental set-up includes a double pass rectangular duct, solar simulator, plenum, temperature measuring devices, pressure measuring devices, and blower. To analyse the impact of artificial roughness it is essential to design and fabricate a double pass rectangular duct utilized in double pass solar air heater. The experimental set-up includes a wooden rectangular duct. The dimensions given to the rectangular duct are 2070 mm × 250 mm × 25 mm. Total height of 50 mm is given to the rectangular duct of double pass air heater. The duct includes an entry region, test region and a minute gap so that the air can move up easily. The entry of the duct has been designed as defined by ASHRAE standards [37] i.e. $5\sqrt{WH}$. The entry region parameters are as follows:

Test section = 1600 mm, gap provided for proper air circulation = 70 mm

The suction of air is done from blower through lower part of double pass rectangular duct. The capacity of blower is 3 HP. This air moves up to upper part of the rectangular duct from the gap provided after/beyond the test region. The exit air then passed through the

flexible pipe which is made up of GI material to the mixing chamber which is known as plenum. The calibrated orifice plate has been inserted in the GI pipe. It has been utilised to find out the mass flow rate of air. A U-tube manometer has been attached to the GI pipe to measure the pressure drop.

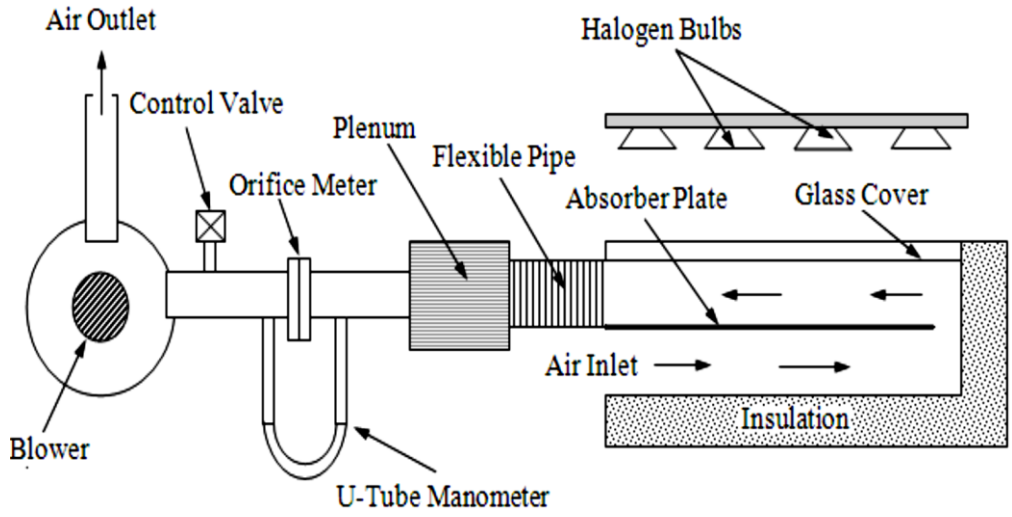

Figure 5.1: Schematic Diagram of experimental set-up

An absorber plate made up of galvanised iron acts as the test section. With the help of ribs the roughness is applied on the lower & upper surfaces of the collector plate. For constant heat flux halogen bulbs are provided. These halogen bulbs acts as solar simulator. The heat flux from the simulator incident on the absorber plate through a transparent cover. The transparent cover is made up of glass. The temperature of test specimen and air heated in the rectangular duct are measured. This is done by using copper-constantan thermocouples and a digital micro-voltmeter. The micro-manometer is used to find the pressure drop across the test section. There are two control valves provided, one of which is at the inlet of blower. The other is at the outlet of the blower. These are used to control the air mass flow rate. The brief description of components are as under.

5.2.1 Solar Air Heater Duct

Fig. 5.2, 5.3 and 5.4 shows the 3-D, sectional, and pictorial view of the double pass solar air heater duct. The cross section of duct is rectangular and is fabricated from the wood. The W/H of the duct is 45.45. The length of the absorber plate/test section is 1600 mm. the rectangular duct is designed according to ASHRAE standards [37] given by $5\sqrt{WH}$. The bottom of the duct is made up of wooden plank having thickness of 19 mm and a plywood

of thickness 6 mm is fixed over it. The other two sides of the duct is made up of wooden plank having thickness of 25 mm. Sunmica laminate of 1 mm thickness has been glued on the top of the plywood to have a smooth surface. A 70 mm gap is provided for proper air circulation after 2000 mm lengh. A glass sheet having 4 mm thickness and 50 mm height is used so that the channel formed is of double pass. This is because the solar rays can be fall easily on to the absorber plate.

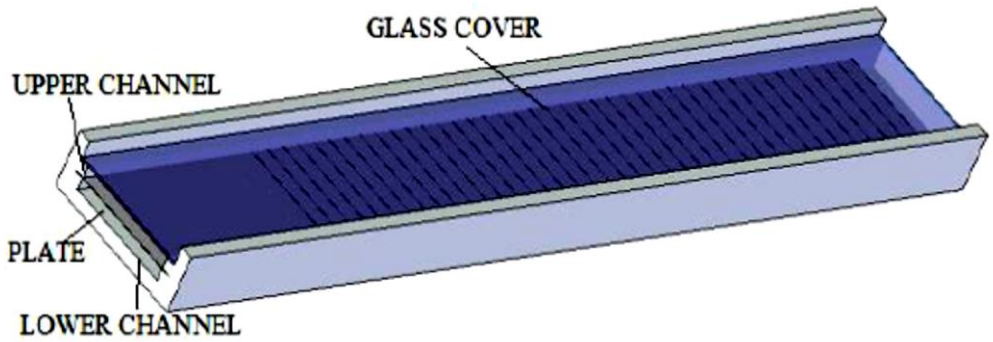

Figure 5.2: Double pass solar air heater duct (3-D view)

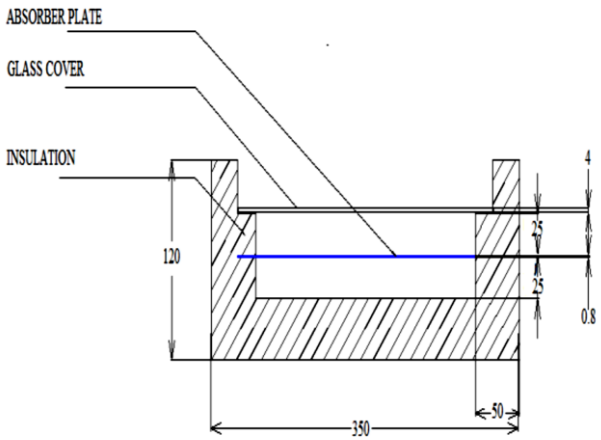

Figure 5.3: Sectional view of duct

Figure 5.4: Pictorial view of solar air duct

5.2.2 Solar Simulator

Fig. 5.5 shows the pictorial view of solar simulator. For both concentrating and non-concentrating applications of solar system these solar simulators have been design. The main aim of solar simulator is to simulate the spectral and spatial solar radiation distribution of sun based radiations into a focal plane of a solar system. Solar simulator is required to get a constant heat flux of 900W/m² fall on to the absorber plate. Solar simulator includes six halogen lamps having intensity of 500W each. These halogen lamps are attached on a stand exactly above the duct. The heat flux from these lamps directly incident over absorber plate. The heat flux intensity is measured by pyrometer. Fig. 5.6 shows the combined assembly of solar duct and solar simulator.

Figure 5.5: Pictorial view of solar simulator

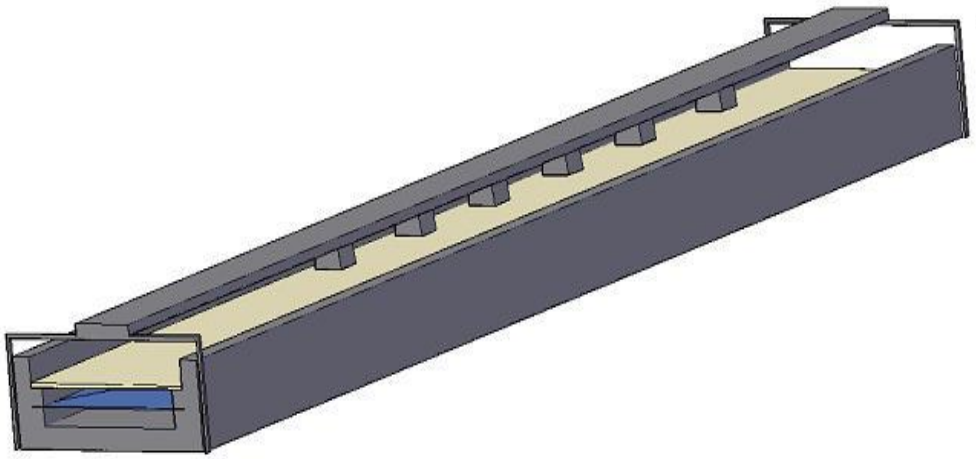

Figure 5.6: Combined assembly of solar simulator and solar air heater channel

5.2.3 Absorber Plate

A pictorial view of discrete W-shaped roughened absorber plate is shown in figure 5.7 and figure 5.8. The absorber plate is made up of galvanised iron. The size of absorber plate is 1600 mm × 250 mm. Discrete W-shaped ribs are provided on both sides of the absorber plate. Top side of the absorber plate is painted black and the bottom side of the absorber plate remains unpainted. The heat flux has been incident in the top surface of the absorber plate and the plate gets heated.

Figure 5.7: Pictorial view of absorber plate (α = 60°)

Figure 5.8: Pictorial view of absorber plate (α = 30°)

5.2.4 Air Handling Equipment

Atmospheric air is sucked by centrifugal blower through the lower channel of the rectangular duct. The capacity of the centrifugal blower is 3 HP, 3-phase, 230 V and 2820 rpm motor. The upper channel or we can say that exit of the duct is connected to the centrifugal blower by a galvanised iron pipe of 80 mm diameter. A calibrated orifice and a plenum is attached to this pipe. At entry and exit of the blower two control valves are provided for the control of rate of flow of air. To reduce the transmission of vibrations from blower to duct a flexible pipe of 600 mm in length is provided between the control valves and orifice plate. Gaskets and seals are provided in all the connections to prevent air leakages.

5.2.5 Instrumentation

5.2.5.1 Pressure Measurement

To measure the pressure difference across the test section a projection manometer is used. The manometer is having the least count of 0.01 mm. It includes a fixed and movable reservoirs. These reservoirs are connected with a transparent tube with flexible tubing. A lead screw is used for the mounting of the movable reservoir. Lead screw having pitch of 1 mm, and a dial gauge having 100 divisions. Each division shows the movement of reservoir of 0.01 mm. The reservoirs are connected with air traps of the duct. The meniscus is maintained at a fixed mark. This is done by moving the moving the reservoir down and up. The movement readings are noted and the difference in pressure is then measured.

5.2.5.2 Temperature Measurement

The temperature of the absorber plate and air was measured with the help of thermocouples. The thermocouples type used in this investigation are copper-constantan (T type) thermocouples. These thermocouples were initially calibrated. Figure 5.10 shows the calibration curve for the thermocouples. Twelve thermocouples were attached on top surface of the absorber plate. The measured temperatures at these points were then averaged to find the mean temperature of the plate. Figure 5.9 shows the location of thermocouples on to the absorber plate. One thermocouple was provided at the inlet of duct

and one thermocouple at the exit of the duct. The inlet and exit temperatures were also averaged to find the mean temperature of the flowing air.

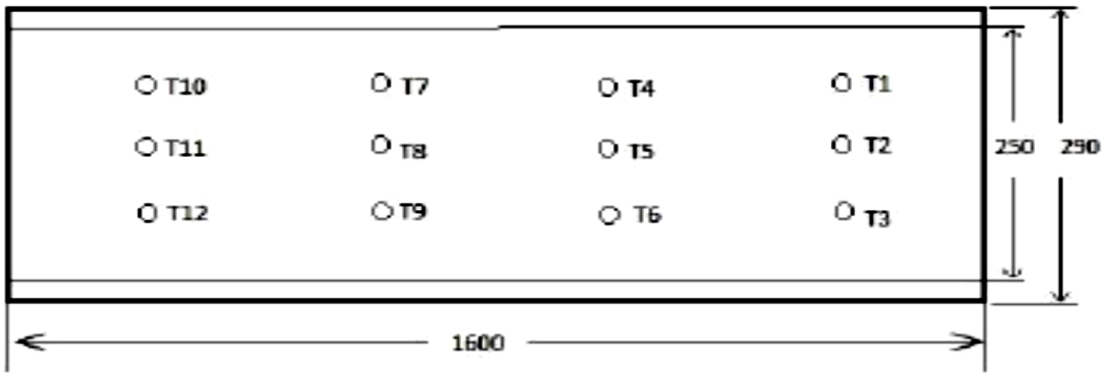

Figure 5.9: Location of the thermocouples on the absorber plate

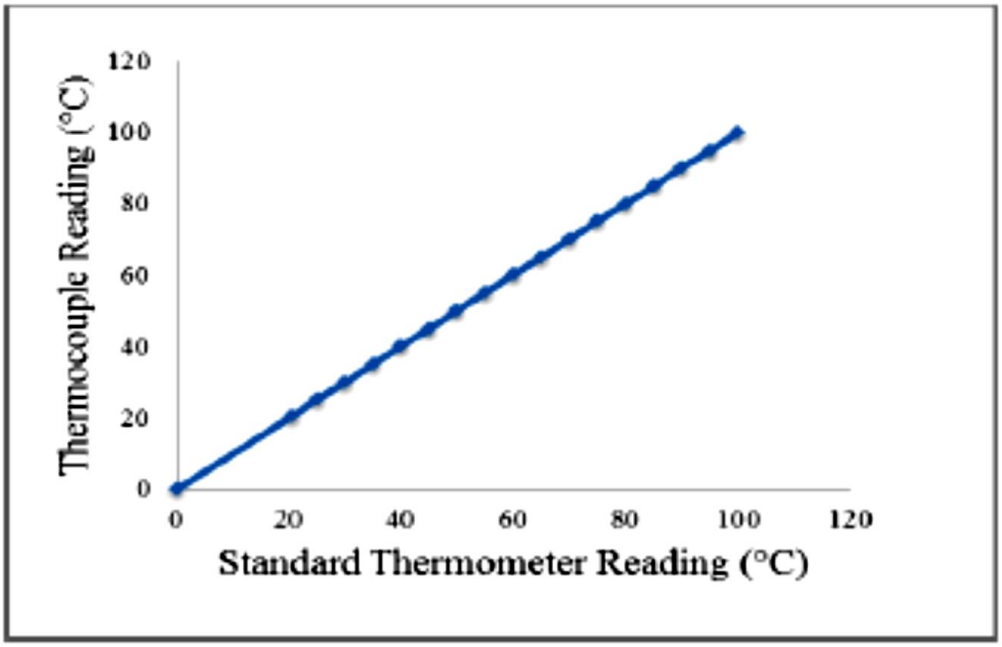

Figure 5.10: Calibration curve for thermocouples

5.2.5.3 Air Flow Measurement

The air flow rate through the duct was measured with the help of concentric orifice plate. This orifice plate was designed, and fabricated. This fabricated orifice plate was then fitted in the galvanised iron pipe of 80 mm diameter in which air was flowing from plenum to the blower. Orifice plate was calibrated against the pitot tube. The coefficient of discharge

value of orifice plate was determined as 0.612. This coefficient of discharge is used to calculate the mass flow rate of the air. To measure the pressure difference across the orifice plate a U-tube manometer was used.

Table 5.1: Description of Equipment Used:

Sr. No.	Equipment	Material	Dimension	Capacity
1.	Solar Air Heater Duct	Wood	2070 × 250 × 25 mm	-
2.	Absorber Plate	GI Sheet	1600 × 250 mm	-
3.	Flexible Pipe	GI	80 mm dia.	-
4.	Flexible Pipe	Plastic	600 mm length	-
5.	Projection Manometer	-	0.01mm LC/ 100 divisions	-
6.	Centrifugal Blower	-	-	3 HP, 3 phase, 230 V and 2820 rpm
7.	Solar Simulator	-	-	900 W/m²
8.	Thermocouple	Copper-constantum	-	-
9.	Glass Sheet	Glass	4 mm – thickness	-

5.3 Roughness Geometry and Range of Parameters

Aluminium ribs are attached on both sides of absorber plate by using glue. These ribs are circular in shape. These ribs are attached in discrete W shape. The height of ribs and the pitch are defined in non-dimensional form. These are mentioned as e/D_h and p/e. The angle of inclination of ribs is referred as angle of attack (α). Table 5.2 shown the range of parameters.

Table 5.2: Range of Parameters

S. No.	Parameter	Range
1.	Aspect Ratio (W/H)	10
2.	Relative Roughness Height (e/D_h)	0.044
3.	Relative Roughness Pitch (p/e)	5-20
4.	Angle of Attack (α)	30°-60°
5.	Reynolds Number (Re)	4000-18000

5.4 EXPERIMENTAL PROCEDURE

It is necessary to inspect the apparatus that there should be no leakage before starting the experimental work. All the entry and exit sections, pipe fittings and duct joints were properly inspected for leakage. These joints, fittings and sections were sealed properly to avoid leakage.

To obtain the appropriate data for the values of heat transfer and friction factor, it was necessary to run the experiment under quassi-static state. The following data were recorded:

1. Temperature of absorber plate at 12 different locations and entering and leaving air temperature through the duct.
2. Pressure drop across the test section.
3. Pressure difference across the orifice plate.

5.5 DATA REDUCTION

The experimental data required to calculate the heat transfer coefficient, friction factor, and Nusselt number have been given below:

5.5.1 Mean Air and Plate Temperature:

The average of temperature of absorber plate at 12 various locations gives the mean temperature of plate, T_p and is given by

$$T_p = \frac{T_5+T_6+T_7+T_8+T_9+T_{10}+T_{11}+T_{12}+T_{13}+T_{14}+T_{15}+T_{16}}{12} \quad (5.1)$$

T_f, bulk mean temp is the arithmetic mean of air temperature at entry and exit region

$$T_f = \frac{T_1+T_2+T_3+T_4}{4} \quad (5.2)$$

5.5.2 Mass Flow Rate of Air ($\dot{m}$):

Mass flow rate of air is calculated by the drop in pressure across the orifice meter, and is given by the following relation

$$\dot{m} = C_d A_0 \sqrt{\frac{2\rho\ (\Delta P_0)}{1-\beta^4}} \quad (5.3)$$

5.5.3. Velocity of Air through Duct (V):

Velocity of air is calculated by the following relation of mass flow rate and the flow area

$$V = \frac{\dot{m}}{\rho W H} \quad (5.4)$$

5.5.4 Hydraulic Diameter (D_h):

The hydraulic diameter of the flow channel is calculated by the following relation

$$D_h = \frac{4A_c}{P} \quad (5.5)$$

5.5.5 Reynolds Number (Re):

The relation of Reynolds number is given by

$$Re = \frac{\rho V D_h}{\mu} \quad (5.6)$$

5.5.6 Friction Factor (f):

Fiction factor is calculated by the Darcy Wiesbach equation. For that pressure difference across the length of test section is measured. The relation is given by

$$f = \frac{2(\Delta P_{duct}) D_h}{4\rho L V^2} \quad (5.7)$$

5.5.7 Heat Transfer Coefficient (h):

The heat transfer coefficient is calculated by

$$h = \frac{Q_u}{A_p(T_p - T_f)} \quad (5.8)$$

Where, "T_p" and "T_f" are the temperature (mean) absorber plate and the fluid i.e. air, respectively, heat transfer rate (Q_u) to the air is given by,

$$Q_u = mC_p(T_o - T_i) \quad (5.9)$$

5.5.8 Nusselt Number (Nu):

The Nusselt number is given by the following relation

$$Nu = \frac{hD_h}{k} \quad (5.10)$$

5.6 VALIDATION OF EXPERIMENTAL SET-UP

Before starting the experiment, the system should be calibrated. The system is tested for validation of instruments and set up. The experimental investigation is done on a conventional flat smooth plate. The flow and heat transfer characteristics are then

calculated by experiment. These experimental values of friction factor and Nusselt number are then compared with the values obtained by modified Blassius equation [38] and Dittus Boelter equation [39] respectively.

Figure 5.11 and Figure 5.12 shows the deviation of experimental value with the predicted value of friction factor and Nusselt number with same value of Reynolds number respectively.

Modified Blassius equation

$$f_s = 2 \times 0.085 Re^{-0.25} \quad (5.11)$$

Dittus-Boelter equation

$$Nu_s = 2 \times 0.024 Re^{0.8} Pr^{0.4} \quad (5.12)$$

The modified Blassius equation as well as Dittus-Boelter equation both multiplied by 2 because of double pass air flow in the rectangular duct.

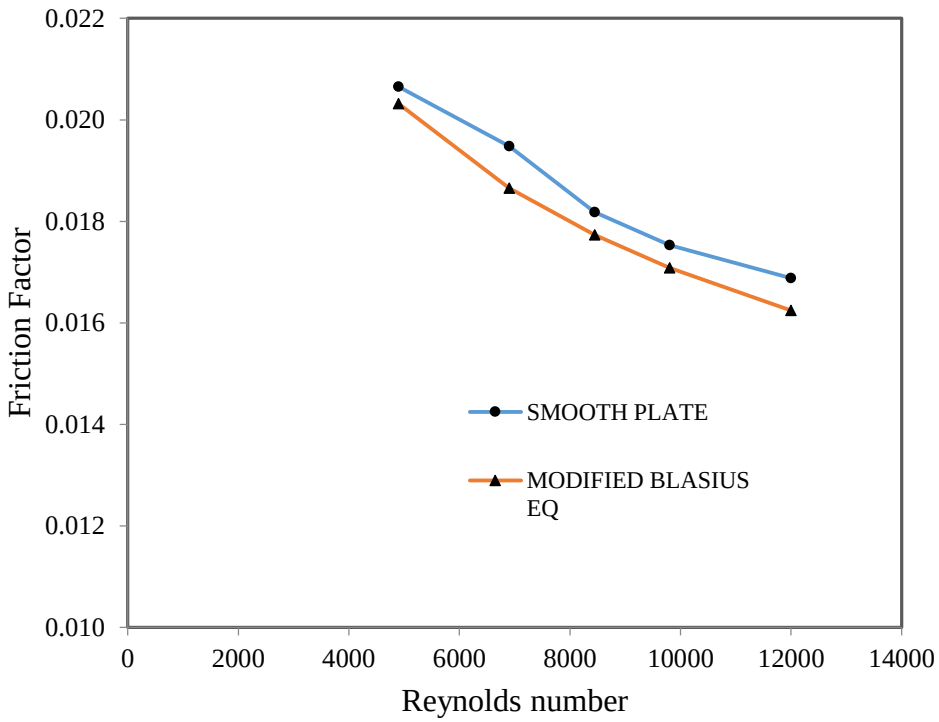

Figure 5.11: Comparison of experimental Friction factor with predicted value of Friction factor for smooth plate

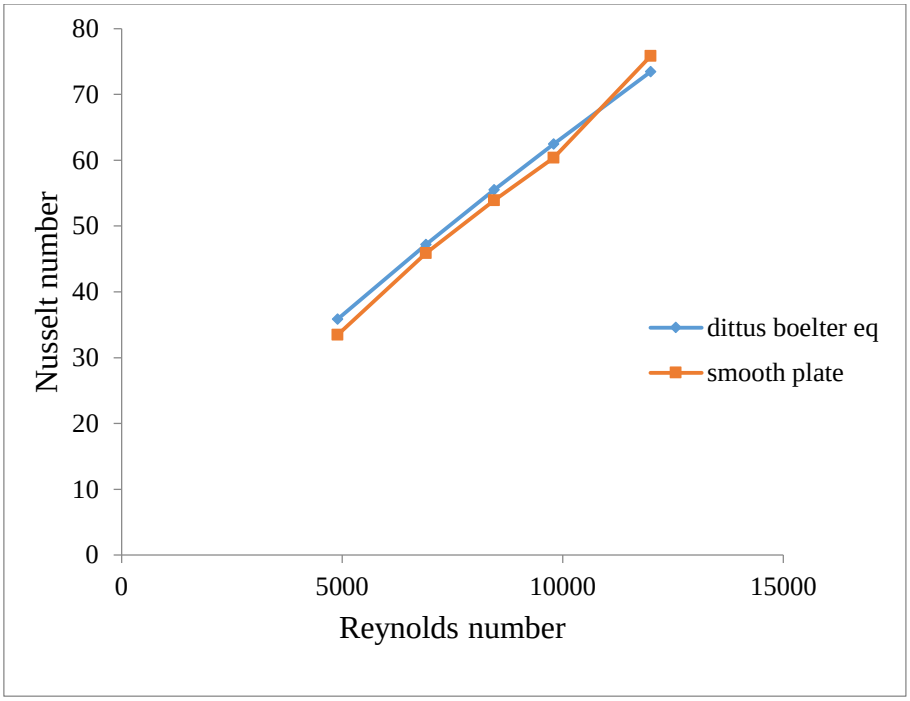

Figure 5.12: Comparison of experimental Nusselt number with predicted value of Nusselt number for smooth plate

It is reported that the maximum variation of experimental values from predicted values of friction factor and Nusselt number found to be 5% and 7.2% respectively. This certified that the data obtained by this experiment is satisfactory.

5.7 UNCERTAINTY ANALYSIS

For uncertainty analysis the proposed method explained by Kline and McClintock [40] has been used. For all the roughned plates maximum uncertainty found were given below

i) Reynolds number (Re) = 2.287%

ii) Nusselt number (Nu) = 4.173%

iii) Friction Factor (f) = 3.308%.

CHAPTER – 6 RESEARCH METHODOLOGY

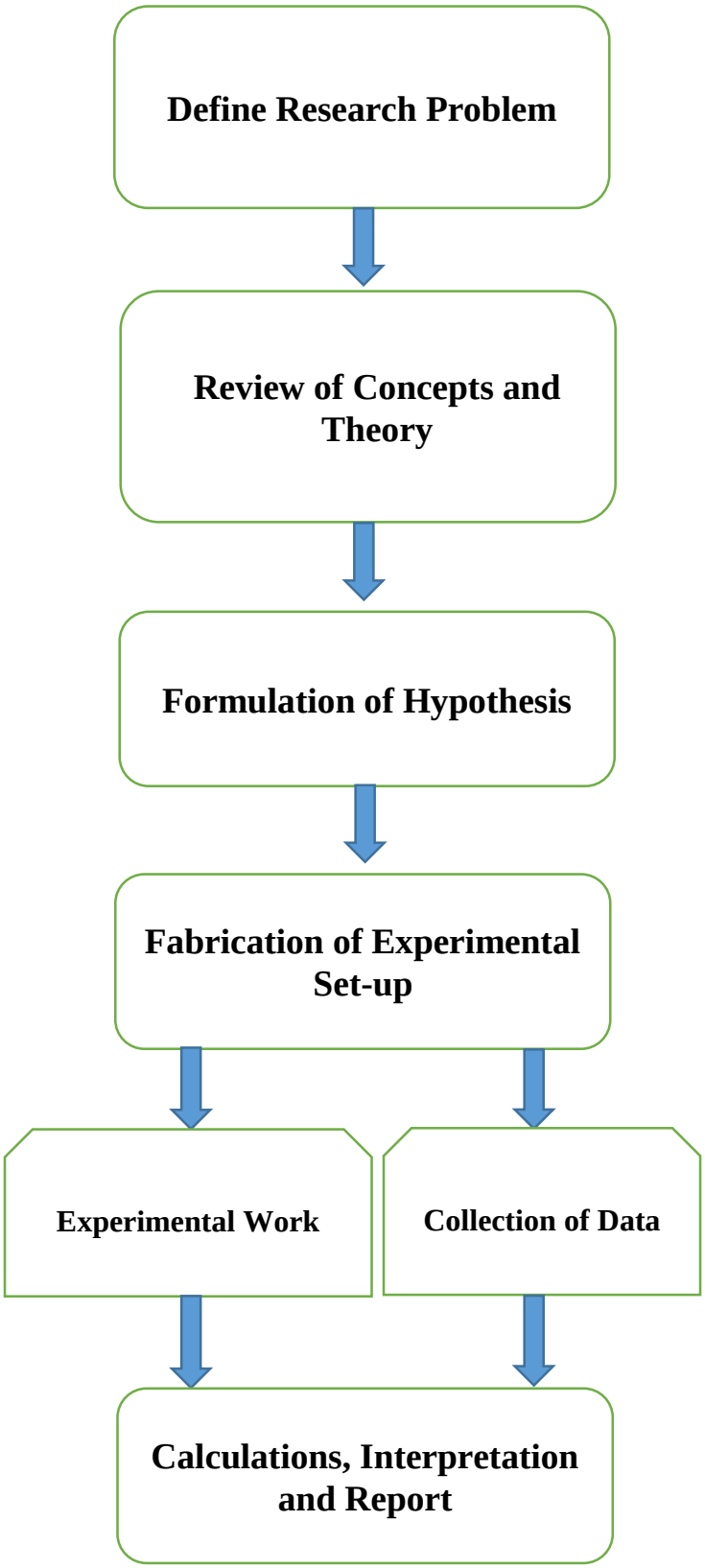

CHAPTER – 7 THERMAL PERFORMANCE

7.1 INTRODUCTION

Solar energy has been used in various applications. These applications are solar air heater, solar cooker, solar dryers. Radiations of sun is converted into heat energy. It is generally called as solar thermal energy (STE). Solar collectors are used for this purpose. Generally there are two types of collectors which are used for conversion of solar energy to heat energy. These collectors are high temperature collectors and low temperature collectors. The efficiency of the solar air heater is low. This is because of low convective heat transfer coefficient. Therefore to increase the efficiency the most common method is to apply artificial roughness on the surface of the absorber plate.

For single pass solar air heater artificial roughness is provided on the lower side of the absorber plate. For double pass solar air heater roughness is provided on the both sides of absorber plate. By doing this the efficiency is increased. The ribs breaks the laminar sub layer. The artificial roughness makes the turbulent flow near the walls in both lower and upper channels. This results in the increase in the heat transfer. The effect of operating parameters and roughness is being observed. A comparison has been done between solar air heaters having roughened absorber plate with the solar air heater having smooth plate. The comparison is done to evaluate the increase in performance of solar air heater due to use of inclined ribs.

7.2 PROCEDURE FOR EVALUATION OF THERMAL EFFICIENCY

The Nusselt number and friction factor were calculated for the absorber plate. Mass flow rate of 0.0122, 0.0173, 0.0214, 0.0247 and 0.0303 kg/s were achieved for each absorber plate. Then each absorber plate was tested for given mass flow rate. The various experimental parameters were recorded by various devices. These parameters are intensity of solar simulators, ambient temperature, air and plate temperatures. This data has been used to determine the thermal efficiency by following procedure:

Step I: Mass flow rate calculation by use of various drop in pressure across the orifice meter with the help of U-tube manometer.

$$\dot{m} = C_d A_0 \sqrt{\frac{2\rho\ (\Delta P_0)}{1-\beta^4}} \quad (7.1)$$

Step II: The heat transfer coefficient is determined by:

$$h = \frac{Q_u}{A_p(T_p - T_f)} \quad (7.2)$$

Where Q_u is the net heat gain and is given by

$$Q_u = mC_p(T_o - T_i) \quad (7.3)$$

Step III: Thermal efficiency is calculated by:

$$\eta_{th} = \frac{Q_u}{A_p I} \quad (7.4)$$

This performance calculation has been done on fixed relative roughness height, various relative roughness pitch and angle of attack.

7.3 THERMAL EFFICIENCY

The thermal efficiency of smooth and roughened absorber plate has been calculated. Figure 7.1 and 7.2 show the effect of roughness and operating parameters.

7.3.1 Effect of Relative Roughness Pitch

Figure 7.1 shows the change of thermal efficiency with Reynolds number. This variation is for the various relative roughness pitch ranges from 5 to 20. The value of relative roughness height and angle of attack is fixed i.e. 0.044 and 60°. It is concluded that maximum thermal efficiency achieved for p/e of 10, after this value thermal efficiency starts reducing. This is because of flow separation explained by Verma and Prasad. [41]

At p/e of 5 the efficiency of roughened plate is less. It is similar to that of smooth plate. This is because of the gap between the ribs is very small. So the plate behave like a smooth plate. The flow does not separated. No reattachment point has been formed.

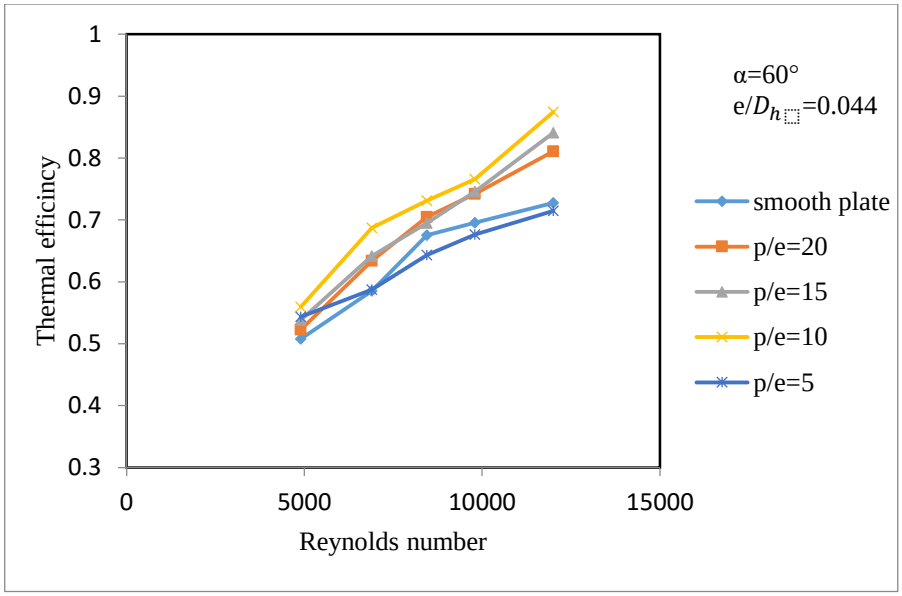

Figure 7.1: Variation of thermal efficiency with Reynolds number for different values of relative roughness pitch and keeping relative roughness height and angle of attack fixed.

7.3.2 Effect of Angle of Attack

Figure 7.2 shows the change of thermal efficiency with Reynolds number. The variation is for the angle of attack varies from 30° to 60°. The values of relative e/D_h and p/e are fixed i.e. 0.044 and 10 respectively. The maximum value of thermal efficiency is achieved at an angle of attack of 60°. The value of thermal efficiency starts decreasing from 60° to 30°

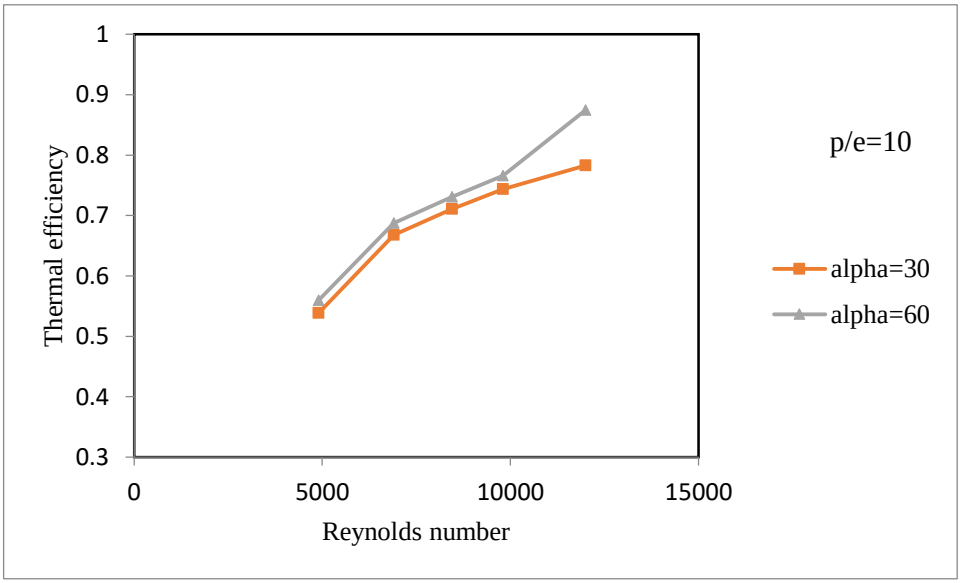

Figure 7.2: Variation of thermal efficiency with Reynolds number for different values of angle of attack and keeping relative roughness height and relative roughness pitch fixed.

7.4 OVERVIEW OF THERMOHYDRAULIC PERFORMANCE

The efficiency of the solar air heater is low. This is because of low convective heat transfer coefficient. This coefficient is between the absorber plate and the flowing air through the duct. So, to enhance the rate of thermal exchange the flow should be turbulent in the vicinity of the heat transfer surface. Hence to make the turbulent flow and to break the laminar sub-layer the artificial roughness is provided on both sides of absorber plate. This results in turbulence in the flow thereby increasing the heat transfer rate.

However, excessive turbulence results in excessive friction losses. Excessive friction losses results in greater power requirement. Therefore to reduce the friction losses to minimum possible level, the turbulence must be generated near the duct wall surface.

7.5 THERMOHYDRAULIC PERFORMANCE OF SOLAR AIR HEATER

Thermohydraulic performance includes the thermal and hydraulic characteristics consideration.

Thermohydraulic performance = Thermal performance + Hydraulic characteristics

The electrical energy is used in pumping operation. According to 2^{nd} law of thermodynamics it has been concluded that a considerable amount of thermal energy is reducing. Hence there is a need of a power. This power is termed as pumping power. It is required to convert in to thermal energy to calculate thermal efficiency. The thermal efficiency is given by:

$$\eta_{th=} \frac{Q_u - \frac{Pm}{C}}{IA_o} \qquad (7.5)$$

Where C = $\eta_F \eta_M \eta_{Tr} \eta_{Th}$.

η_F = Efficiency of Fan or Blower.

η_M = Efficiency of the Electrical Motor used for Driving Fan.

η_{Tr} = Efficiency of Electrical Transmission.

η_{Th} = Thermal Conversion Efficiency of Power Plant.

By calculations the value of conversion factor comes out to be 0.2.

7.5.1 Determination of Thermal Energy Gain (Q_u)

The rate of useful thermal energy gain for roughened solar air heater is given by:

$$Q_u = \mathrm{m}C_p(T_o - T_i) \quad (7.6)$$

7.5.2 Determination of Mechanical Power (P_m)

The mechanical power is required to drive the air through the duct. It is given by:

$$P_m = VA(\Delta P_d) \quad (7.7)$$

The pressure drop across the duct is given by:

$$\Delta P_d = \frac{2fLV^2\rho}{D_h} \quad (7.8)$$

The equivalent diameter is given by:

$$D_h = \frac{4 \times \left(\frac{1}{2}\right) \times W \times H}{3 \times W} \quad (7.9)$$

Putting the values of eq. 8.8 and 8.9 in eq. 8.7, we get:

$$P_m = 1.5WV^2fL\,\rho \quad (7.10)$$

7.6 Energy Balance for a Solar Air Heater

It has been noticed that at low Reynolds number there is an increase in the rate of useful energy. At higher Reynolds number the curve is also become flatter. However at lower Reynolds number the increase rate in consumption of power is low. In case of smooth plate if Reynolds number is high then the net gain in energy steeply increases. The rate of energy

collected becomes almost constant. The rate of net energy gain might disappear. Hence, as Reynolds number increases the consumption of power and collection of useful energy becomes equal.

7.7 RESULTS AND DISCUSSION

The effective efficiency of smooth and roughened absorber plate has been found out by method explained by Cortes and Piacentini [42]. The effects of different roughness parameters have been shown in figure 7.3 and 7.4. It is concluded from these figures that the roughened absorber plate results in better efficiency as compared with smooth plate.

It is also concluded from the figure that as Reynolds number increases the efficiency also increases. But after a certain value of Reynolds number the efficiency start decreasing. This is because of the decrease in the heat collected and increase in the pump work. The maximum value is obtained at the e/D_h of 0.044, p/e of 10, and α of 60°.

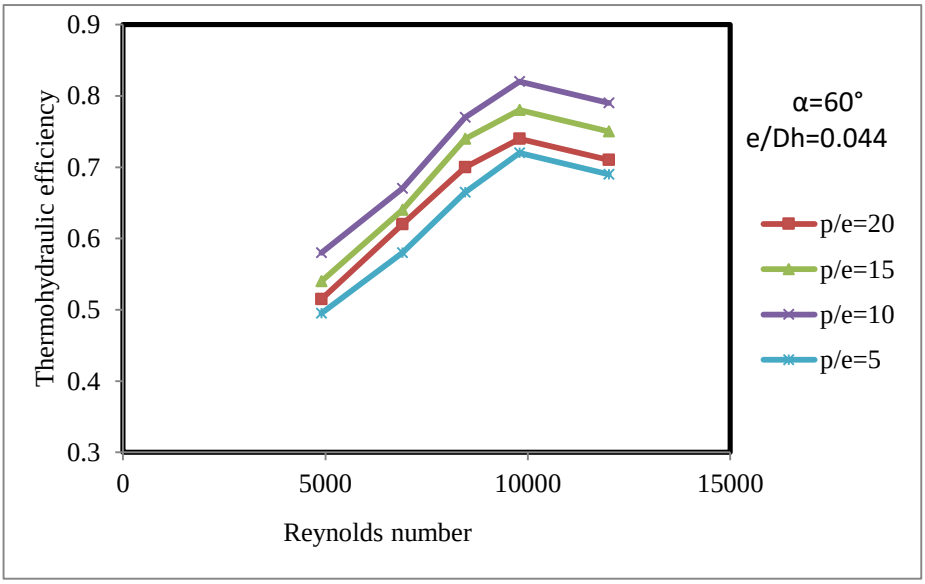

Figure 7.3: Variation in the effective efficiency as a function of Reynolds number for different values of relative roughness pitch and fixed value of angle of attack and relative roughness height.

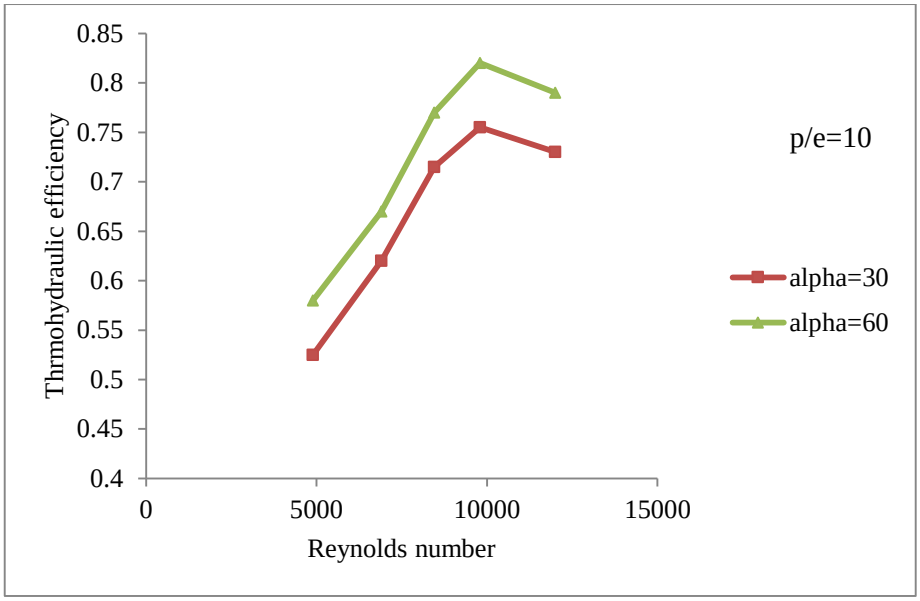

Figure 7.4: Variation in the effective efficiency as a function of Reynolds number for different values of angle of attack and fixed value of relative roughness height and relative roughness pitch.

Therefore generally it is concluded from above graphs that for double pass solar air heater the thermal as well as Thermohydraulic efficiencies are increases up to a certain point. The maximum efficiency is at an angle of attack of 60° and p/e of 10. At p/e of 5 the plate behaves as a smooth plate. This is because the ribs attached very close to each other. Hence no vortex regions are formed. Generally more than 20% increase in the thermal as well as Thermohydraulic efficiencies as compared with the smooth plate have been obtained.

CHAPTER – 8 RESULTS

8.1 INTRODUCTION

Roughness induce turbulence i.e. flow when interact with element (both above and below) changes to turbulent. It happens due to:

- Separation of flow
- Formation of reattachment points
- Breaking of laminar sub-layer

This process leads to elevated heat transfer parameters such as: a) pumping power b) friction factor and c) heat transfer coefficient. Thus, parameters associated with roughness as well as operating parameters are detailed mainly:

- relative roughness height (e/D_h)
- relative roughness pitch (p/e)
- angle of attack (α) and
- Reynolds number

Comparison between roughened and smooth surface is made. It has been concluded that both Nusselt number as well as friction factor value has increased for double pass solar air heater.

8.2 RESULTS AND DISCUSSION

8.2.1 Nusselt number (Nu)

For altered alignments of roughness geometry, Nusselt number (Nu) and Reynold number characteristics are plotted. The Nusselt number is an increasing function of Reynolds number. At (p/e) = 10 and (α) = 60° maximum Nusselt number is obtained. Variation of other parameters is shown below:

8.2.1.1 Effect of Relative Roughness Pitch (p/e)

The variation in Nusselt number for (p/e) values of 5, 10, 15 and 20, α & e/D_h of 60° and 0.044 respectively. Figure 8.1 shows that Nusselt number increases for different values of relative roughness pitch as Reynolds number increases. The value for p/e = 10 is maximum for Nusselt number. The flow separates in rib downstream. However, does not reattaches for lesser value of relative roughness pitch (p/e) than 10 as in p/e=5.

Reattachment point finds maximum heat transfer. Hence, maximum heat transfer occurs at p/e = 10. As the value of relative roughness pitch (p/e) elevates reattachments are lowered causing lesser heat transfer. Figure 8.2 shows Nusselt number variation and relative roughness pitch (p/e) for varying Reynolds number. The value of angle of attack (α) and relative roughness height (e/D_h) remains constant. For lesser value of Reynolds number negligible change in Nusselt number is seen. However, it becomes significant in higher range of Reynolds number.

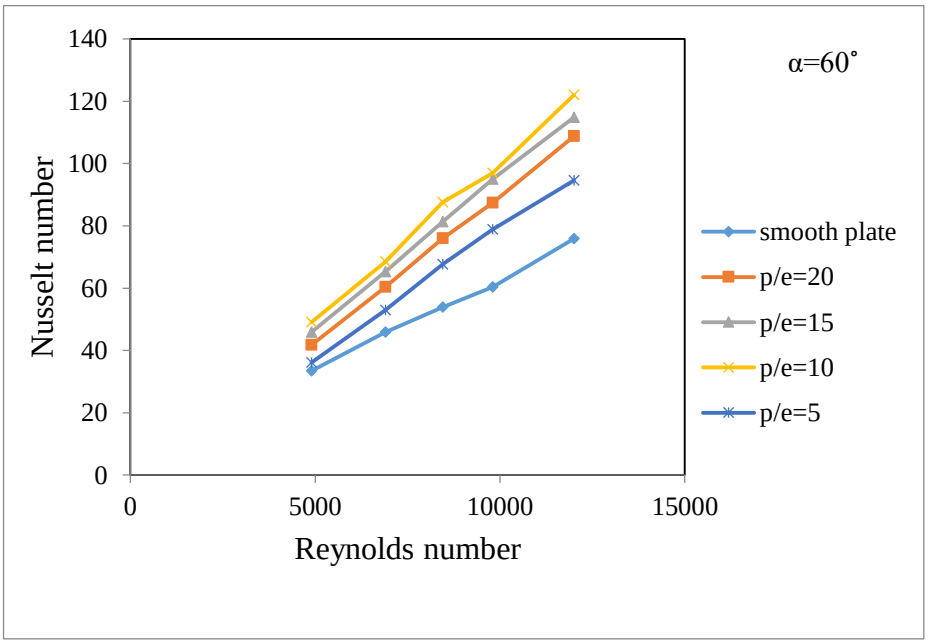

Figure 8.1: Variation of the Nusselt number with the Reynolds number for different values of p/e and for fixed e/D_h = 0.044 and α = 60°.

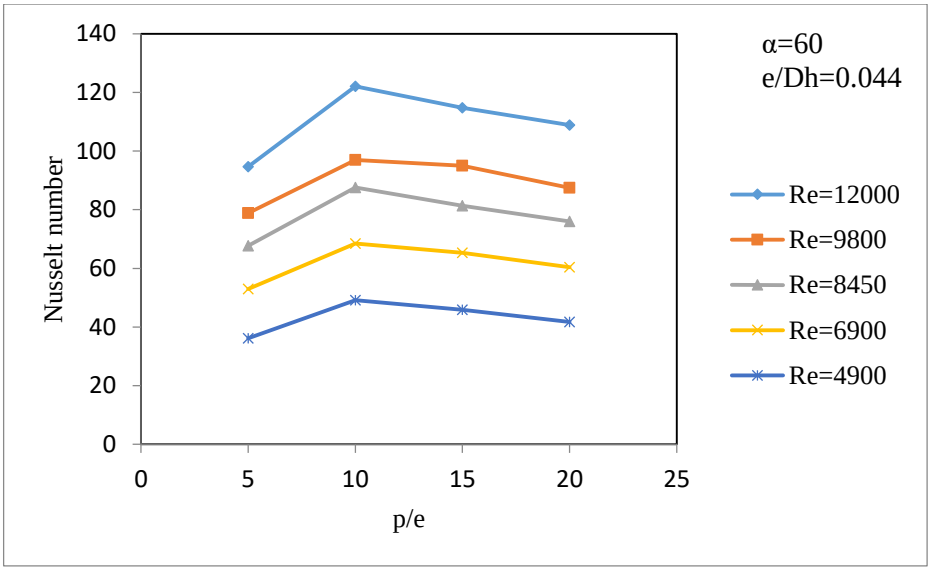

Figure 8.2: Variation of the Nusselt number as a function of relative roughness pitch for various Reynolds number and for fixed relative roughness height and angle of attack.

8.2.1.2 Effect of Angle of Attack (α)

Figure 8.3 angle of attack (α) varies 30° and 60° keeping relative roughness height (e/D_h) of 0.044 and relative roughness pitch (p/e) of 10 as constant. Nusselt number is directly proportional to angle of attack. This happens as the ribs create anti-rotating secondary flow along test section length as by Hans et al. [43] and Varun et al. [44]. Heat transfer is achieved maximum for angle of attack (α) of 60°. This decreases as angle of attack up to 30° due to lower anti-rotating secondary flow.

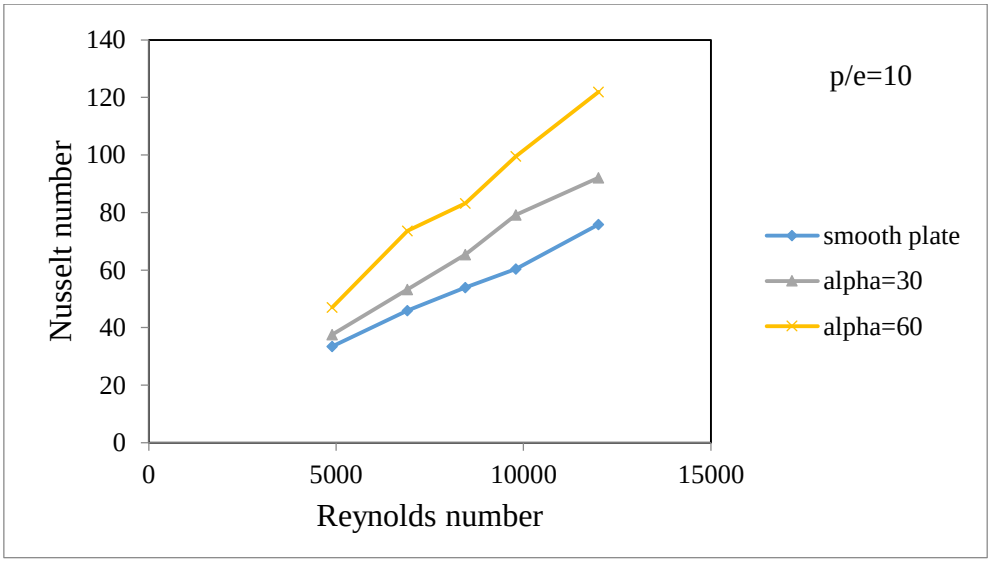

Figure 8.3: Variation of the Nusselt number with the Reynolds number for different values of alpha and for fixed e/D_h = 0.044 and p/e = 10.

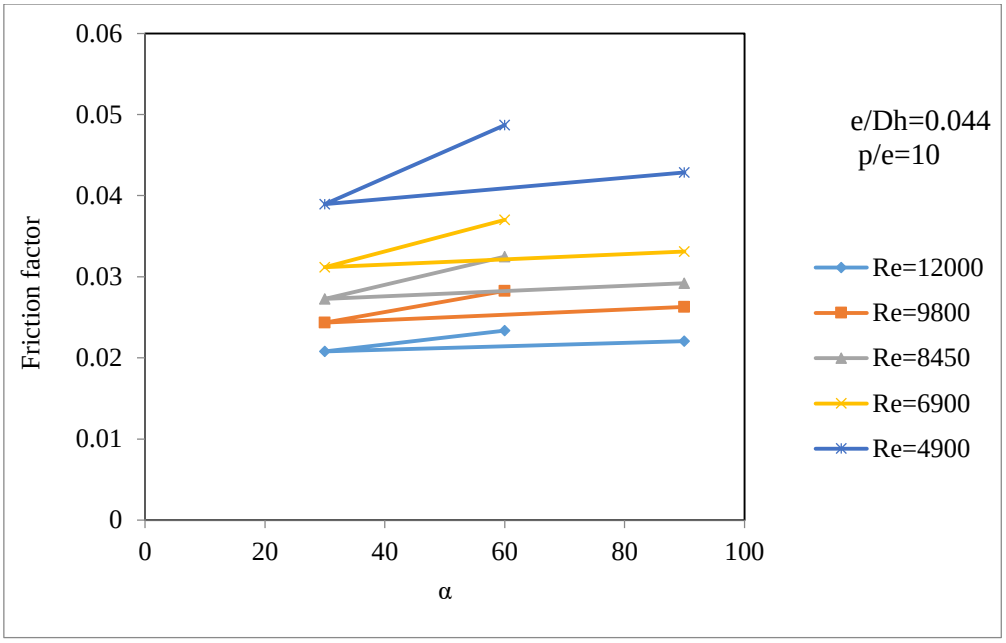

Figure 8.4: Variation of the Nusselt number as a function of angle of attack for different values of Reynolds number and for fixed relative roughness height and relative roughness pitch.

8.2.2 Friction Factor (f)

Effect of different roughness geometry orientations are discussed for friction factor. The friction factor behaves inversely with Reynolds number. However, relative roughness height of (e/D_h) 0.044 finds maximum friction factor at an angle of attack (α) of 60 & relative roughness pitch (p/e) of 10.

8.2.2.1 Effect of Relative Roughness Pitch (p/e)

Figure 8.5 shows the variation of relative roughness pitch (p/e) of 5, 10, 15 and 20 keeping e/D_h of 0.044 & α of 60° constant. Friction factor reduces with Reynolds number. Maximum value is achieved at p/e = 10. In Figure 9.5 the Friction factor decreases linearly for all p/e.

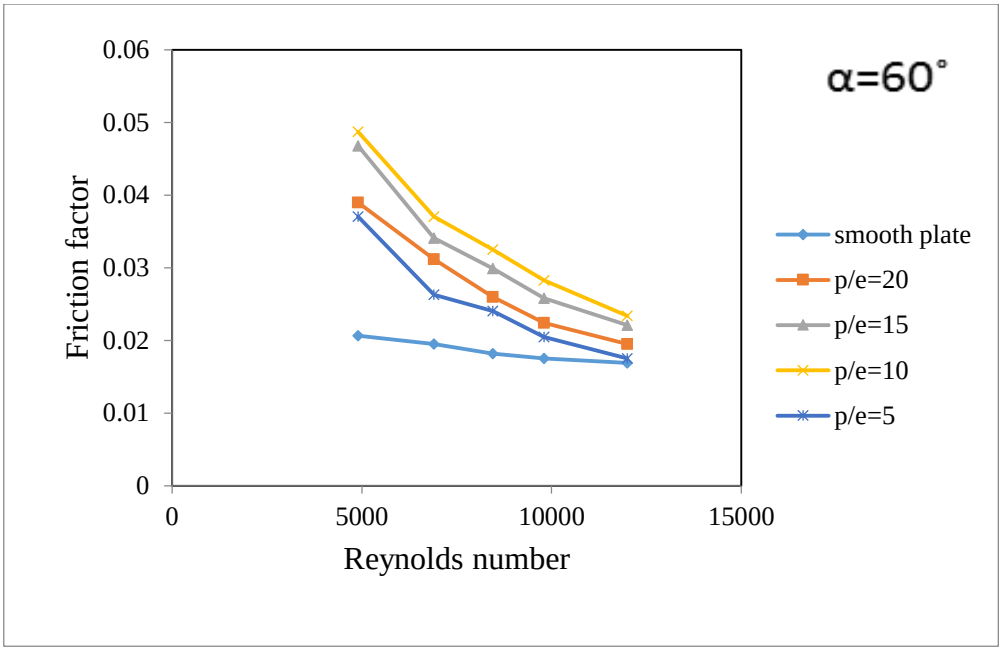

Figure 8.5: Variation of friction factor with the Reynolds number for different values of p/e and for fixed e/Dh =0.044 and α =60°.

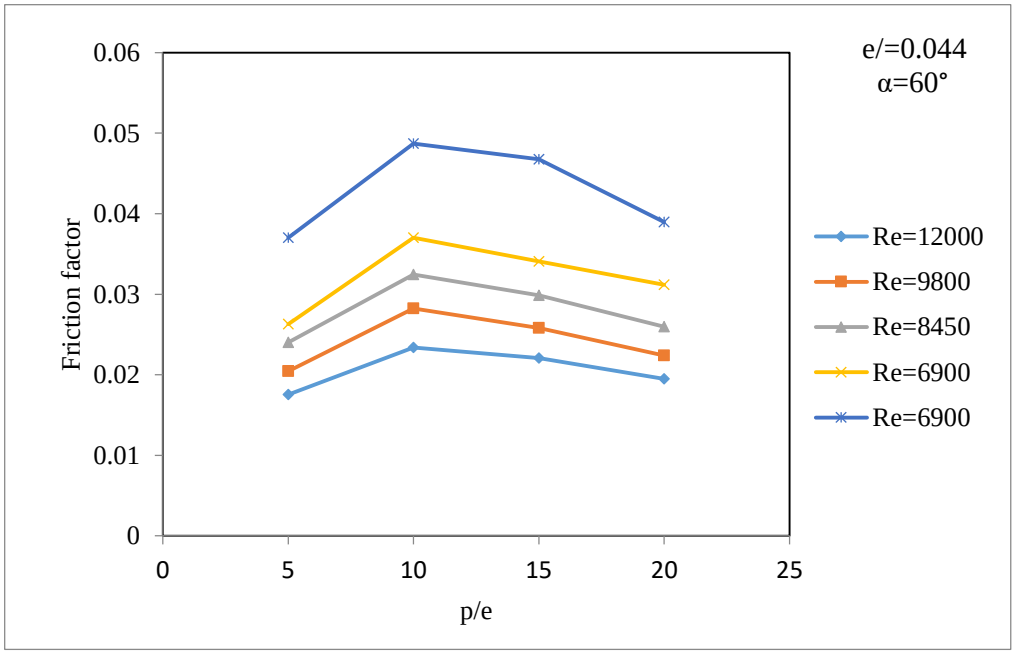

Figure 8.6: Variation of the friction factor as a function of relative roughness pitch for different values of Reynolds number and for fixed relative roughness height and angle of attack.

8.2.2.2 Effect of Angle of Attack (α)

Figure 8.7 shows variation of angle of attack (α) of 30° and 60°. The value of p/e of 10 and e/D_h of 0.044 is kept constant. It is found that maximum friction factor is obtained at 60° due to larger anti-rotating secondary flow at high α. The variation of friction factor as a

function of angle of attack for different values of Reynolds number. For fixed value of e/D_h and p/e has been shown in Figure 8.7.

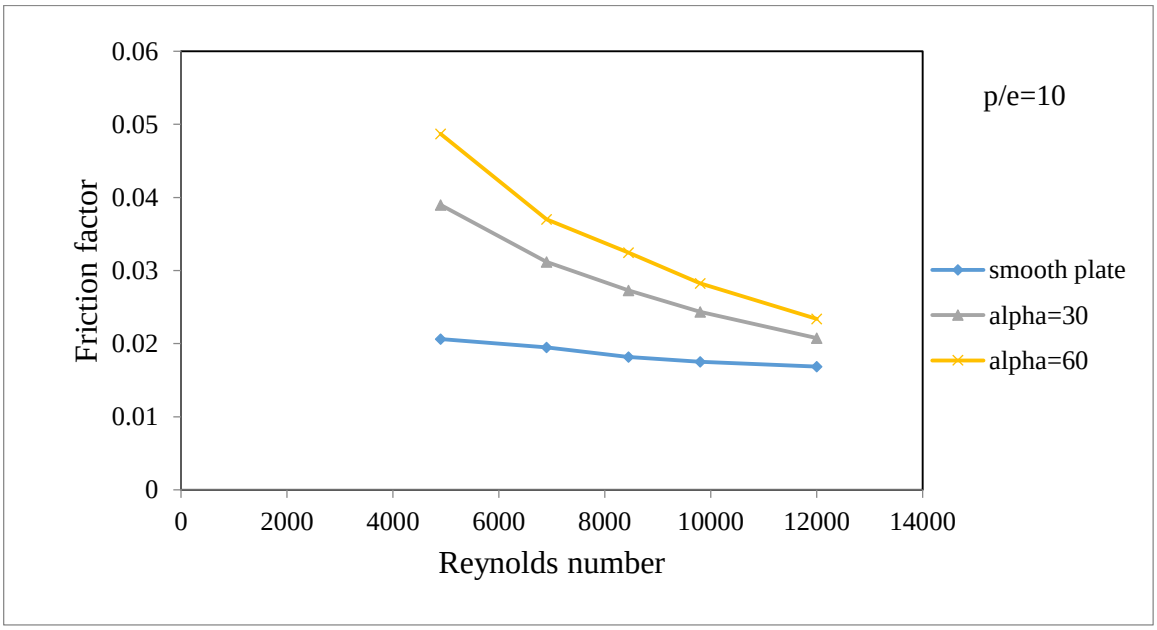

Figure 8.7: Variation of friction factor with the Reynolds number for different values of alpha and for fixed e/Dh =0.044 and p/e=10.

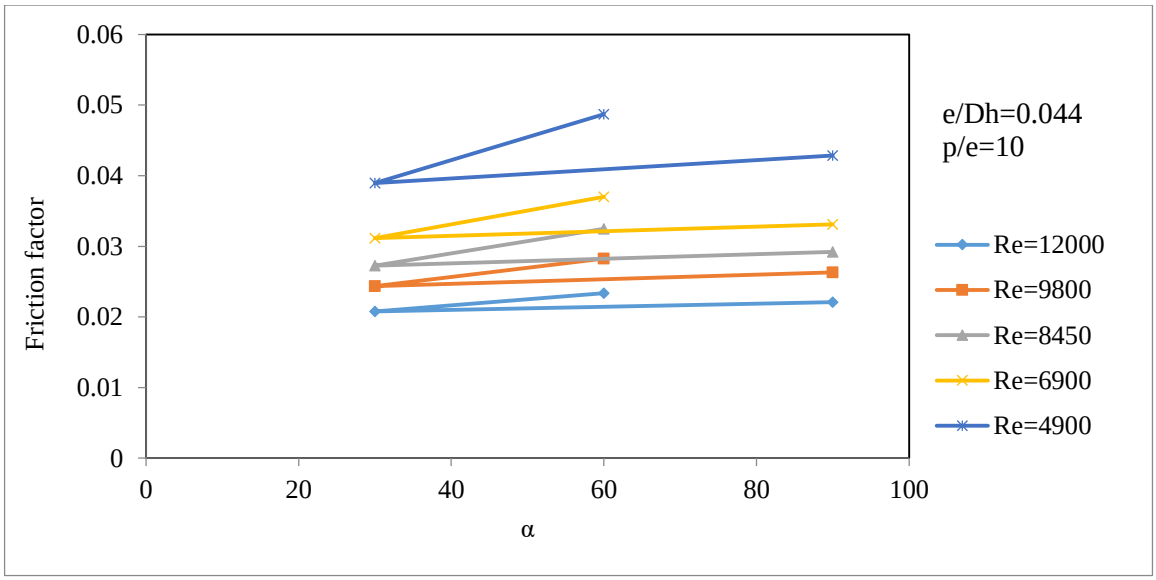

Figure 8.8: Variation of the friction factor as a function of angle of attack for different values of Reynolds number and for fixed relative roughness height and relative roughness pitch.

CHAPTER – 9 CONCLUSION AND SUMMARY

Experiments are carried out on Double pass solar air heater using discrete W-shaped ribs on both sides of the absorber plate and then compare it with that of Single pass solar air heater of the same geometry. It is found that double pass solar air heater has more thermal as well as Thermohydraulic efficiency than single pass solar air heater under same angle of attack and pitch conditions. The thermal efficiency of approximately 87% is being recorded for double pass solar air heater. The thermo-hydraulic efficiency of approximately 84% is being recorded for double pass solar air heater. Hence it is concluded that the thermal and Thermohydraulic efficiencies for double pass solar air heater having discrete W shaped ribs on both sides of the absorber plate are more as compared with double pass solar air heater having continuous W shaped ribs. Also this type of solar air heater is having better efficiency as compared with single pass solar air heater having same geometry.

REFERENCES

[1] G. D. Rai, Non-Conventional energy sources, Khanna publications, New Delhi, 1997.

[2] G. K. Ghosh, Solar energy, The infinite source, Ashish publishing house, New Delhi 1991.

[3] Ministry of New and Renewable Energy, Government of India, http://www.mnes.nic.in.

[4] Goswami, D. Y. Kreith, F. and Kreider, J.K., Principles of Solar Engineering, Taylor and Francis, 2003.

[5] Sen, Z. Energy and Climate Change, Solar energy fundamentals and modeling techniques, Verlag London limited: Springer; 2008.

[6] Duffie and Beckman, Solar engineering of thermal processes (second edition), A Wiley Inter science publication, John Wiley and sons, Inc., New York, 1980.

[7] Garg, H.P. and Prakash, J. P., Solar Energy- Fundamentals and Applications, Tata McGraw-Hill, New Delhi.

[8] Satcunanathan, S. and Deonarine, S., A two pass solar air heater, Solar Energy 15(1) (1973), 41-49.

[9] Malhotra, A., Garg, H. P. and Rani, U., The effect of gap spacing on convective losses in flat plate collectors, Proceeding of National Solar Energy Convection, I.I.T Bombay (1979), 52-56.

[10] Malhotra, A., Garg, H.P. and Rani, U., Minimizing convective heat losses in flat plate solar collectors, Solar Energy 25(6) (1980), 521-526.

[11] Bevill, V.D. and Brandt, H., A solar energy collector for heating air, Solar Energy 12 (1968), 19-29.

[12] A. Saxena, N. Agarwal, and G. Srivastava, “Design and performance of a solar air heater with long term heat storage,” *Int. J. Heat Mass Transf.*, vol. 60, no. 1, pp. 8–16, 2013.

[13] S. Singh, S. Chander, and J. S. Saini, “Heat transfer and friction factor correlations of solar air heater ducts artificially roughened with discrete V-down ribs,” *Energy*, vol. 36, no. 8, pp. 5053–5064, 2011.

[14] S. Kumar and R. P. Saini, “CFD based performance analysis of a solar air heater duct provided with artificial roughness,” *Renew. Energy*, vol. 34, no. 5, pp. 1285–1291, 2009.

[15] Varun, R. P. Saini, and S. K. Singal, “Investigation of thermal performance of solar air heater having roughness elements as a combination of inclined and transverse ribs on the absorber plate,” *Renew. Energy*, vol. 33, no. 6, pp. 1398–1405, 2008.

[16] Brij Bhushan, Ranjit Singh, Nusselt number and friction factor correlations for solar air heater duct having artificially roughened absorber plate, Solar energy 85 (2011) 1109-1118.

[17] M. Samiev, “Efficiency of solar plate air heaters,” *Appl. Sol. Energy*, vol. 44, no. 4, pp. 258–261, 2008.

[18] P. Dhiman, N. S. Thakur, A. Kumar, and S. Singh, “An analytical model to predict the thermal performance of a novel parallel flow packed bed solar air heater,” *Appl. Energy*, vol. 88, no. 6, pp. 2157–2167, 2011.

[19] K. Patel, S. Soni, and S. Travadi, “‘ Comparative Study of Double Pass Solar Air Heater with Solar Air Heater with Baffles & With Longitudinal Fins ,’” pp. 2790–2794.

[20] S. Chamoli, R. Chauhan, N. S. Thakur, and J. S. Saini, “A review of the performance of double pass solar air heater,” *Renewable and Sustainable Energy Reviews*, vol. 16, no. 1. pp. 481–492, 2012.

[21] K. Patel, S. Soni, and U. Soni, “A Review to Enhance the Efficiency of Double Pass Solar Air Heater,” no. February, pp. 712–715, 2015.

[22] A. Kumar, “Analysis of heat transfer and fluid flow in different shaped roughness elements on the absorber plate solar air heater duct,” *Energy Procedia*, vol. 57, pp. 2102–2111, 2014.

[23] Pongjet Promvonge, Chinaruk Thianpong, “Thermal Performance Assessment of Turbulent Channel Flows over Different Shaped Ribs, ” International Communications in Heat and Mass Transfer 35 (2008) 1327 - 1334.

[24] A. Kumar, R. P. Saini, and J. S. Saini, “Development of correlations for Nusselt number and friction factor for solar air heater with roughened duct having multi v-shaped with gap rib as artificial roughness,” *Renew. Energy*, vol. 58, no. 12, pp. 151–163, 2013.

[25] N. S. Deo, S. Chander, and J. S. Saini, “Performance analysis of solar air heater duct roughened with multigap V-down ribs combined with staggered ribs,” *Renew. Energy*, vol. 91, pp. 484–500, 2016.

[26] R. K. Ravi and R. P. Saini, “A review on different techniques used for performance enhancement of double pass solar air heaters,” *Renew. Sustain. Energy Rev.*, vol. 56, pp. 941–952, 2016.

[27] S. Singh and P. Dhiman, “Thermal performance of double pass packed bed solar air heaters - A comprehensive review,” *Renew. Sustain. Energy Rev.*, vol. 53, pp. 1010–1031, 2016.

[28] S. S. Krishnananth and K. Kalidasa Murugavel, “Experimental study on double pass solar air heater with thermal energy storage,” *J. King Saud Univ. - Eng. Sci.*, vol. 25, no. 2, pp. 135–140, 2012.

[29] Raheleh Nowzari, Nima Mirzaiei, L.B.Y. Aldabbagh “Finding the best configuration for a solar air heater" Energy Conversion and Management 100 (2015) 131–137.

[30] R. Nowzari, L. B. Y. Aldabbagh, and N. Mirzaei, “Experimental Study on Double Pass Solar Air Heater With Mesh Layers As Absorber Plate,” *Int. J. Electron. Mech. MECHATRONICS Eng.*, vol. 3 Num 4, pp. 673–68.

[31] A. A. El-Sebaii, S. Aboul-Enein, M. R. I. Ramadan, S. M. Shalaby, and B. M. Moharram, “Thermal performance investigation of double pass-finned plate solar air heater,” *Appl. Energy*, vol. 88, no. 5, pp. 1727–1739, 2011.

[32] A. P. Omojaro and L. B. Y. Aldabbagh, “Experimental performance of single and double pass solar air heater with fins and steel wire mesh as absorber,” *Appl. Energy*, vol. 87, no. 12, pp. 3759–3765, 2010.

[33] Avdhesh Sharma, Varun, Prashant Kumar, and Gaurav Bharadwaj, “Heat transfer and friction characteristics of double pass solar air heater having V-shaped roughness on the absorber plate”, JOURNAL OF RENEWABLE AND SUSTAINABLE ENERGY 5, 023109 (2013).

[34] M. R. I. Ramadan, A. A. El-Sebaii, S. Aboul-Enein, and E. El-Bialy, “Thermal performance of a packed bed double-pass solar air heater,” *Energy*, vol. 32, no. 8, pp. 1524–1535, 2007.

[35] B. Bhushan and R. Singh, “A review on methodology of artificial roughness used in duct of solar air heaters,” *Energy*, vol. 35, no. 1, pp. 202–212, 2010.

[36] D. P. Singh, M. K. Tated, and S. Dogra, “Experimental analysis of heat transfer and friction factor in double pass solar air heater by using discreate ribs on the absorber plate,” *Int. J. Sci. , Technol. Manag.*, vol. 4, no. 1, pp. 677–684, 2015.

[37] ASHARAE Standard 93–77. Method of testing to determine the thermal performance of Solar Air Heater, New York 1997; 1–34.

[38] Kays W.M., Perkin H. Forced convection internal flow in ducts. In: Rohsenow W.M., Hartnett I.V, editors, Handbook of Heat Transfer. New York:McGraw-Hill.

[39] Bhatti MS, Shah RK. Turbulent and transition flow convective heat transfer. In: Kakac S, Shah RK, Aung W, editors. Handbook of Single-phase Convective Heat Transfer. New York: John Wiley and Sons, 1987.

[40] Kline, S.J. and McClintock, F.P., Describing uncertainties in single-sample experiments, Mech. Engg. (75) (1953) 3-8.

[41] Prasad, B.N. and Saini, J.S., Effect of artificial roughness on heat transfer and friction factor in a solar air heater, Solar Energy 41 (1988), 555-560.

[42] Cortes, A. and Piacentini, R., Improvement of the efficiency of a bare solar collector by means of turbulent promoters, Applied Energy 36 (1990), 253-261.

[43] Hans, V.S., Saini, R.P. and Saini, J.S., Performance of artificially roughened solar air heaters – A review, Renewable and Sustainable Energy Reviews 13 (2010), 1854-1869.

[44] Varun, Saini, R.P. and Singal, S.K., A review on roughness geometry used in solar air heaters, Solar energy 81 (2007), 1340-1350.